



ENHANCEMENT OF DIRECT TORQUE CONTROL OF THREE PHASE INDUCTION MOTOR



MAY 24, 2020

1. Abstract:

Three-phase induction motor is one of the common-used motors in industrial and commercial sectors nowadays. Hence, giving a specific speed to the motor to operate at it quickly with a tolerable error while there is a large torque load or friction on the wheels or at the output of the motor is not an easy task to handle, such as the case in speed cruiser in some of the cars. As a result, Direct Torque Control is an important task that research tackles and seeks for its development better each day. The conventional direct torque control utilized a small PI control to compensate the difference between the required speed and the actual speed. In addition, as we are controlling to maintain a torque load and to achieve a required speed, we have to also control the magnetic flux of the stator as well, in case the speed is above the rated speed. So, in this report the performance of direct torque control will be examined by the conventional way and two other controllers based on sliding mode control theory. The difference between the two controllers based on sliding mode control is only the change of the sliding surface required to push the error to it until stabilizing. The comparison between the performance between the controllers will be examined carefully and will enable us a useful insight of the principle of controlling such induction machines. After deciding the model and the types of controllers used, a Matlab/Simulink model is conducted to show our results and validate our analysis by observing the performance of the proposed controllers. Furthermore, some recommendations for the future work are provided that may guide other researchers working in the same field.

2. Introduction:

There are many types of motor such as DC motors, Single-Phase AC motors, and Three-Phase AC motors. It is well-known that the Three-Phase AC motors is one of the best motors in terms of power and efficiency. However, it more complex to be controlled. As a result, sensor-less control of induction motor drive has received wide attention in the industry in last decades [1]. This returns back to many advantages for the induction motor such as less maintenance and rugged construction, and simultaneously the development of less expensive and fast controllers. The progress of sensor-less drives can be considered to have begun around three decade ago by Blascbke [2]. This concept, now called as field-oriented control (FOC), was a huge turn in the field of electrical drives, then it becomes well established and accepted by the industry. But this method has some disadvantages like dependent on machine parameters, complexity such as referencing the transformations needed, that will be discussed later in the next chapter. Therefore, there was a need for a new strategy that can produce high performance similar to FOC with reduced complexity. Direct torque control (DTC) by Tkahashi [3] for low and medium power application and direct self-control by Depenbrack [4] for high power application are the two strategies increasingly being used in the industry. The DTC was proposed as an alternative to the vector control in the middle of 1980s for AC machine control [5]. In DTC, torque and flux are controlled independently by selecting the optimum voltage space vector for the entire switching period and the errors are maintained with in the hysteresis band. Though DTC has high dynamic performance, it has few drawbacks such as vibrations and acoustic noise due to torque ripple and power loss due to current and flux ripple. As mentioned earlier, DTC objective is possible to control the stator flux and torque directly, the stator flux and the torque are controlled by selecting the appropriate inverter state. The results obtained previously can be tabulated in the so-called optimum switching table [6].

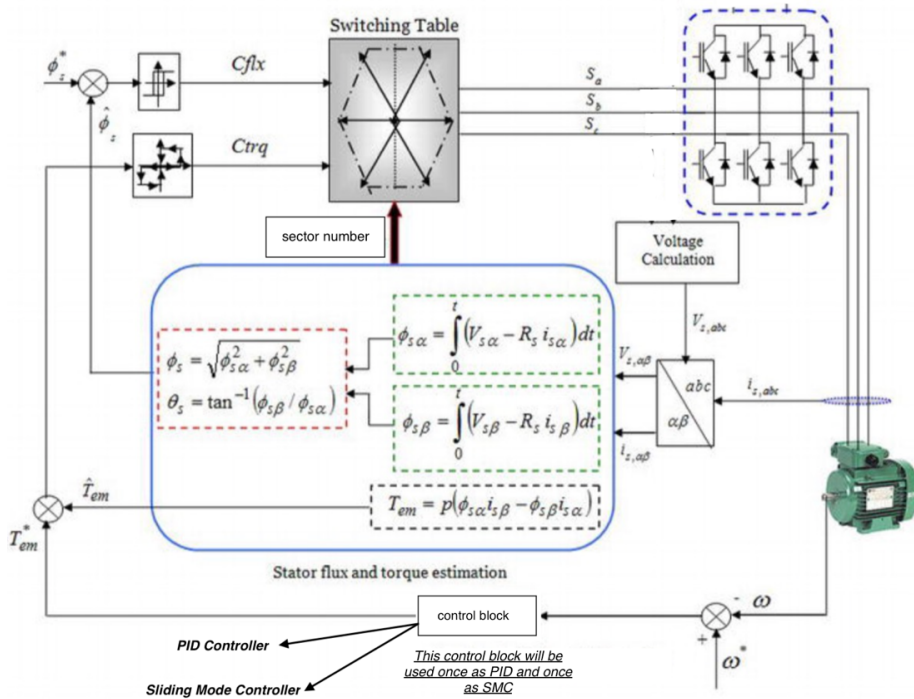


Figure.1 full picture of DTC of IM.

As shown in figure 1, this is the full picture of what all the project revolves around. There is a desired flux and torque required from the controllers to compensate their deviation from the current Torque and flux from the estimator. Then there is the switching table, which was called above “optimum switching table” to generate a certain pulse to the 6 inverters to control the voltage that will be sent to the IM. Also, another technique is widely used associated with DTC is the v/f control technique which has almost the same components as DTC but with different control output that keeps the ratio between volt/frequency constant. In the next chapters we will see each component individually and its modelling technique(s) as well.

3. Modelling of Induction Motor:

In order to begin our analysis, an inductor motor model must be specified which will be a squirrel cage 3 phase induction motor with a star connected one. As the DTC deals with the stationary frame only, so the concern will be for the stationary frame specifically. However, the rotor frame will be required for other visualizing in the results. So, the three-phase squirrel cage induction motor is modeled in the stationary reference frame, as shown in figure 2, and transformed to d-q axes instead of the conventional 3-phase axes.

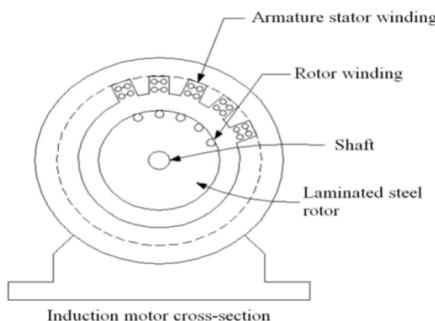


Figure. 2. Induction motor cross-section [6]

When a three phase voltage is applied to the stator winding terminals, three phase balanced currents flow in the armature windings and consequently a rotating magnetic motive force (MMF) field is yielded .This field rotates at synchronous speed (N_s) in revolution per minute.

$$N_s = \frac{120f}{P}, \text{ where}$$

f: supply frequency
P: number of poles in the motor

By faraday's law, this rotating stator magnetic field induces voltages in the rotor windings causing balanced currents to flow in the short circuited rotor. An electromagnetic torque (T_e) is produced due to the interaction between the stator and rotor rotating magnetic fields. The difference between the rotor speed and the stator speed (synchronous speed) defines the per unit slip (s),

$$s = \frac{W_s - W_r}{W_s} \text{ where}$$

W_s : Synchronous speed in rad/sec
 W_r : Rotor speed in rad/sec

At the steady state, the speed of rotor is zero, the slip is equal to unity. However, when the speed of the rotor is equal to the synchronous speed, the slip will be equal to zero, in this case no torque is produced. So, the slip ranges between 0 and 1, as shown in figure 3, the torque speed characteristics of IM.

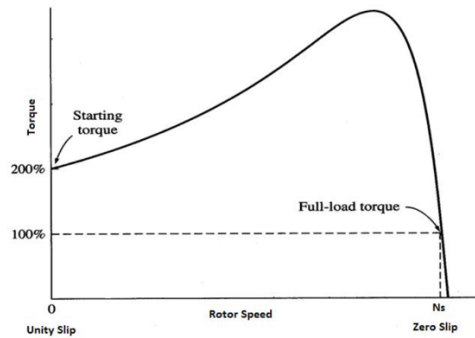


Figure. 3. Torque speed characteristics of IM [6]

All variables of the motor might be referred to a specific frame for modelling. This means that IM can be modelled in different ways depending on the reference frame selected. In this project, the stationary frame is taken as a reference for modelling such as modeled by Alnasir, Z.A. et al. [6]. IM models at stator and rotor frames are explained in details in the book of Induction motor control design [7].

IM stator current is formulated as a vector with its real element in direct axis (d-axis) and its imaginary element in quadrature axis (q-axis). The d-axis current is used to control the rotor flux while the output torque is controlled by the q-axis current. In other words, flux and torque are independently controlled, as

mentioned above in the introduction the topology of DTC. Fig.4 illustrates the dq axis and the expressions of current and voltage in that axis [6].

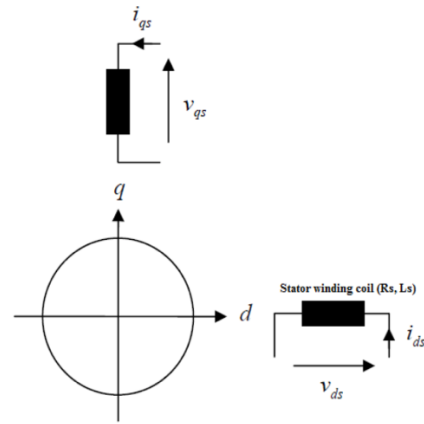


Figure. 4. d-q axes in the stator

So, as derived by the past researchers in the book of Induction motor control design [7], the equivalent circuits of the IM in the d-q axes are shown in figure 5.

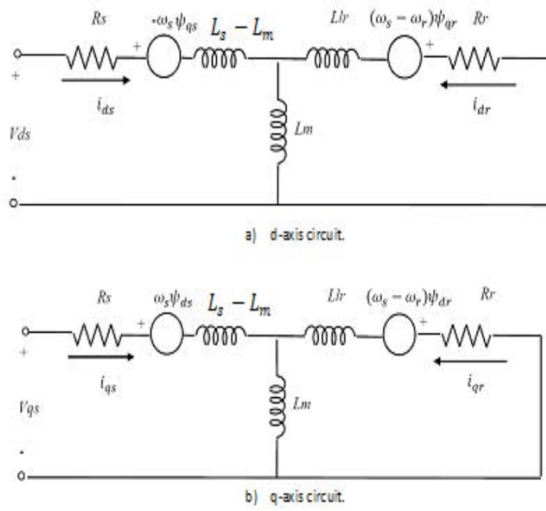


Figure. 5. The d-q

In the beginning, some assumptions must be stated clearly to make this model accurate:

- 1: The air gap between stator and rotor is uniformly distributed and hence stator and rotor windings are in sinusoidal distribution.
- 2: The motor is running at steady state constant speed.
- 3: The motor is initially relaxed.

The representation for this circuit will be done in state space representation system to check its observability and controllability easily.

$$\dot{X} = AX + BU$$

The variables in the d-q circuits are as follows:

ψ_{ds}, ψ_{qs} : d-axis and q-axis stator flux respectively,
 ψ_{dr}, ψ_{qr} : d-axis and q-axis rotor flux respectively,
 i_{ds}, i_{qs} : d-axis and q-axis stator current respectively,
 i_{dr}, i_{qr} : d-axis and q-axis rotor current respectively,
 V_{ds}, V_{qs} : d-axis and q-axis stator voltage respectively,

Assuming zero initial motor speed, the state variables and A, B matrices are as follows.

$$X = \begin{bmatrix} i_{qs} \\ i_{ds} \\ i_{qr} \\ i_{dr} \end{bmatrix}, \quad U = \begin{bmatrix} V_{qs} \\ V_{ds} \\ 0 \\ 0 \end{bmatrix}$$

$$B = \frac{1}{K} \begin{bmatrix} L_r & 0 & -L_m & 0 \\ 0 & L_r & 0 & -L_m \\ -L_m & 0 & L_s & 0 \\ 0 & -L_m & 0 & L_s \end{bmatrix}, \quad K = L_s L_r - L_m^2$$

$$A = \frac{1}{K} \begin{bmatrix} R_s L_r & W_s L_s L_r - W_r L_m^2 & -R_r L_m & 0 \\ W_r L_m^2 - W_r L_s L_r & R_s L_r & 0 & -R_r L_m \\ -R_s L_m & 0 & R_r L_s & W_r L_s L_r - W_s L_m^2 \\ 0 & -R_s L_m & W_s L_m^2 - W_r L_s L_r & R_r L_s \end{bmatrix}$$

Another set of equations including the stator and rotor fluxes are required for DTC. The stator flux and the torque are the state variables which need to be estimated and controlled in DTC as will be seen later.

$$\begin{aligned} \frac{d}{dt} \psi_{ds} &= -R_s i_{ds} + w_s \psi_{qs} + V_{ds} \\ \frac{d}{dt} \psi_{qs} &= -R_s i_{qs} - w_s \psi_{ds} + V_{qs} \\ \frac{d}{dt} \psi_{dr} &= -R_r i_{dr} + (w_s - w_r) \psi_{qr} \\ \frac{d}{dt} \psi_{qr} &= -R_r i_{qr} - (w_s - w_r) \psi_{dr} \end{aligned}$$

$$\begin{aligned} \psi_{ds} &= L_s i_{ds} + L_m (i_{ds} + i_{dr}) = L_s i_{ds} + L_m i_{dr} \\ \psi_{dr} &= L_r i_{dr} + L_m (i_{ds} + i_{dr}) = L_r i_{dr} + L_m i_{ds} \\ \psi_{dm} &= L_m (i_{ds} + i_{dr}) \\ \psi_{qs} &= L_s i_{qs} + L_m (i_{qs} + i_{qr}) = L_r i_{qs} + L_m i_{qr} \end{aligned}$$

$$\begin{aligned}\psi_{qr} &= L_{ir}i_{qr} + L_m(i_{qs} + i_{qr}) = L_r i_{qr} + L_m i_{qr} \\ \psi_{qm} &= L_m(i_{qs} + i_{qr})\end{aligned}$$

Hence, all of the model of our motor is done and can be utilized in our system, all of these equations will be represented in our model as one block which is the “IM”, as shown in figure 1, and the observability and controllability checks for this models can be found in details by Alnasir, Z.A et al [6], all the Simulink screenshots and codes will be available in the appendix.

4. Space Vector Pulse Width Modulation:

The Space Vector Pulse Width Modulation (SVPWM) method is an advanced, computation-intensive PWM method and possibly the best among all the PWM techniques for variable frequency drive application [8,9]. Because of its superior performance characteristics, it has been finding widespread application in recent years [9].

The SVPWM method is about transforming a DC voltage to 3-phase voltages by changing the switching frequencies of 6 alternating switches (inverters), as shown in Figure 6.

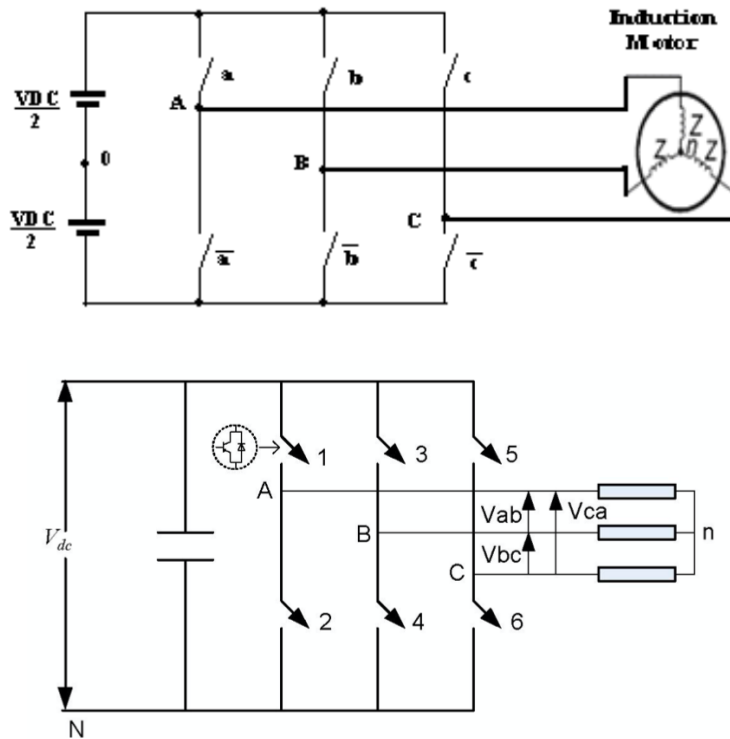


Figure. 6. 3-Phase Voltage Source Inverter

In this method, a fixed dc input voltage is given to the inverter and a controlled ac output voltage is obtained by adjusting the on and off periods of the inverter components. However, there are some constraints that should be considered, that one switch must be on in every leg of the inverters (A,B,C) and only one switch is ON in every leg, so turning on both of them or none of them is not allowed, these rules are validated by giving each switch a signal and the other switch in the same leg is its complimentary signal.

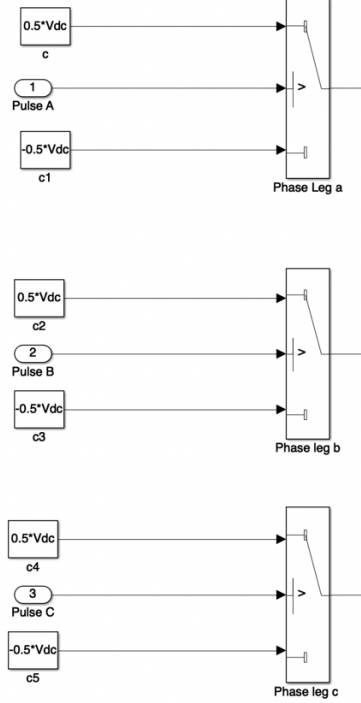


Figure 7. Simulink model of the switches' signals (provided by SVPWM)

Phase-to-neutral voltages of a star-connected load are most easily found by defining a voltage difference between the starpoint (n) of the load and the negative rails of the dc bus N. Then, by observing different conditions of switches, then we can derive the different phase-to-neutral voltages that will be sent to the motor for operating, then starting by the following correlation (for the three phases) [10]:

$$\begin{aligned} v_A &= v_a + v_{nN} \\ v_B &= v_b + v_{nN} \\ v_C &= v_c + v_{nN} \end{aligned} \quad (1)$$

Since the phase voltages in the middle of star connected leads to zero, then it yields to zero:

$$v_{nN} = (1/3) * (v_A + v_B + v_C) \quad (2)$$

Then by substituting (2) in (1):

$$\begin{aligned} v_a &= (2/3)v_A - (1/3) * (v_B + v_C) \\ v_b &= (2/3)v_B - (1/3) * (v_A + v_C) \\ v_c &= (2/3)v_C - (1/3) * (v_A + v_B) \end{aligned}$$

As shown in figure 6,

$$\begin{aligned} v_a &= (2/3) * v_A - (1/3) * (v_B + v_C) \\ v_b &= (2/3) * v_B - (1/3) * (v_A + v_C) \\ v_c &= (2/3) * v_C - (1/3) * (v_A + v_B) \end{aligned}$$

These equations are modeled in the Simulink model as shown in figure 8, outputting the Van, Vbn, and Vcn to the star-connected Induction motor:

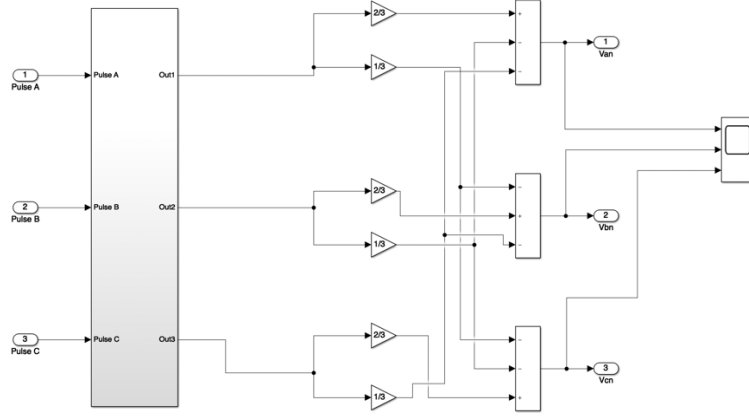


Figure. 8. Simulink model of the supplying voltage to the IM (these outputs from subsystem are from submodel represented in figure 7)

So, the switching table is as shown in the next table for the different switching conditions:

Name	A	B	C	V_{An}	V_{Bn}	V_{Cn}
V_0	0	0	0	0	0	0
V_1	1	0	0	$2V_{DC}/3$	$-V_{DC}/3$	$-V_{DC}/3$
V_2	1	1	0	$V_{DC}/3$	$V_{DC}/3$	$-2V_{DC}/3$
V_3	0	1	0	$-V_{DC}/3$	$2V_{DC}/3$	$-V_{DC}/3$
V_4	0	1	1	$-2V_{DC}/3$	$V_{DC}/3$	$V_{DC}/3$
V_5	0	0	1	$-V_{DC}/3$	$-V_{DC}/3$	$2V_{DC}/3$
V_6	1	0	1	$V_{DC}/3$	$-2V_{DC}/3$	$V_{DC}/3$

Table. 1. Inverters' output [10]

The shown states can be configured as vector, which is well-known for many of researches for better visualization for the different sectors of voltages as shown in the figure 9:

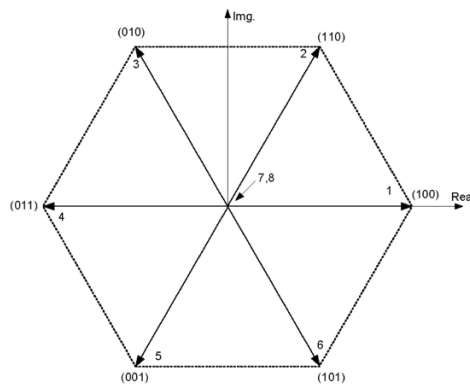


Figure. 9. Phase Voltage Space Vector

As shown in figure 9, there are 6 sectors for different basic vectors for the output voltage from the inverter to the motor. It is pretty obvious that 7,8 are the two cases of [0,0,0] or [1,1,1] which is lead to 0 output voltage.

The choice of which voltage to choose for the switches of the inverters is based upon which sector we are already in, flux's error, and torque's error, in addition to generated frequency in constant v/f technique. After that, based on these values we are choosing which vector to choose as shown in figure 10.

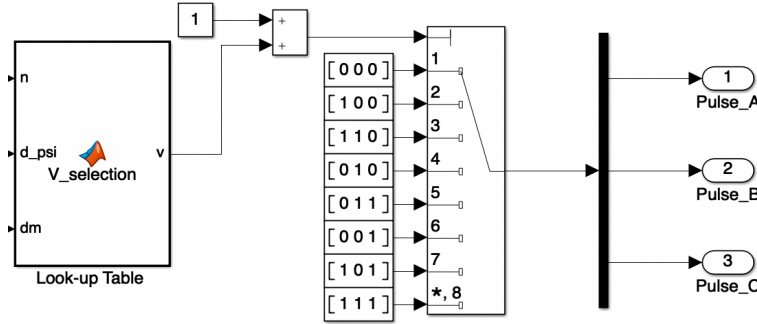


Figure. 10. The look up table for choosing vectors

The only difference between the analytical equations (table shown above) and the Simulink model is adding 1 for the output. This addition is only because that the multiport switch's indexing starts from 1 and not zero, so the output is just shifted from 0 → 7 to 1 → 8.

The full details of determining the frequencies of the switches and the complete analysis of vectors from SVPWM can be found in [6,10], as our main aim is not the SVPWM but the controlling techniques to send signals to the SVPWM, utilizing the SVPWM was just an “voltage source inverter” to our Induction motor. The details of controlling which voltage vector to output is given by the following table:

Error status of		Sector no.					
ψ_s	T_e	1 θ_{s1}	2 θ_{s2}	3 θ_{s3}	4 θ_{s4}	5 θ_{s5}	6 θ_{s6}
0	1	110	010	011	001	101	100
	0	111	000	111	000	111	000
	-1	011	001	101	100	110	010
1	1	100	110	010	011	001	101
	0	000	111	000	111	000	111
	-1	001	101	100	110	010	011

Table.2. The Look-up table from inside [6]

This table decides which voltage vector will be provide a sufficient compensation to stabilize the motor, the stator flux angle in addition to the torque and flux hysteresis status are used to determine the suitable stator flux sector in order to apply the correct voltage vector to the induction motor operating under DTC. Table I lists the switching vectors in the different stator flux sectors [6].

5. Simulink's simulations using different control techniques for DTC:

There are many control techniques for controlling an induction motor, this paper is focusing on direct torque technique but with different controller blocks. DTC is not a novel method, but an old one, but its feasibility increases by development of control theory. The conventional one was based on a PI controller to generate the torque input to the look up table, and relay for flux hysteresis controller, which is sufficient. As a result, this project is to determine the effect of applying sliding mode control with linear sliding surface and non-linear sliding surface (integral sliding surface). In addition to that, results from V/f is acquired to compare the results between the three different approaches.

Also, we are mainly controlling the speed by the means of torque, we are constrained to control under the rated speed only, so we are giving a flux reference constant by 1.1 wb. As a result, we have to do field weakening with the following equation [11] to be able to achieve the required speed(s) above the base speed.

The field weakening strategy of the stator flux reference ($1/\omega_r$), where ω_r is the rotor's speed, and given by this equation, which is used only in case the required speed is higher than the rated one's [11]:

$$\phi_s^* = \phi_{s, \text{rated}} \omega_{\text{base}} |\omega_r|^{-1}$$

In our model, $\omega_{\text{base}} = 100 \pi$, so after implementing this field weakening in our model, it opens for our project a new gate to controlling the speed above the rated one, that will be verified by the results in the next sub-sections.

Controlling any system always requires a feedback from the plant, which is the IM in our case. They are usually sensors providing the sufficient feedback signals for our controllers. However, in any simulation, they are always replaced by either a model of a certain sensor or an estimator. In our simulations, we are using "Stator Flux and Torque Estimator". As shown in Figure 11, this estimator is taking the voltages and the currents of the IM and estimates the stator's torque and flux in order to decide the control action based on the estimated current states. As the analysis shown by M. Shady et al [12], the equations of the estimated torque and flux as follows, where P is the number of poles in the motor, :

$$T_e = \frac{3}{2} \left(\frac{P}{2} \right) (\psi_{sd} i_{sq} - \psi_{sq} i_{sd})$$

$$\psi_{sd} = \int v_{sd} - R_s i_{sd} dt$$

$$\psi_{sq} = \int v_{sq} - R_s i_{sq} dt$$

$$|\bar{\psi}_s| = \sqrt{(\psi_{sd}^2 + \psi_{sq}^2)}$$

So, these equations are implemented in our Simulink model and here is a screenshot of our Simulink model for this estimator:

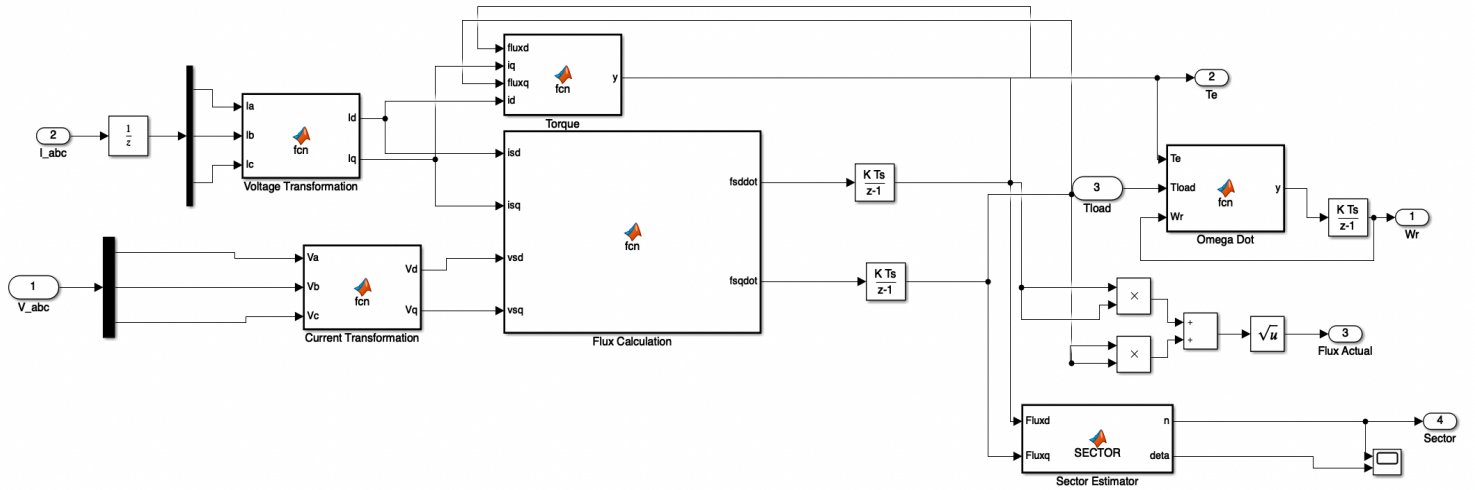


Figure. 11. Simulink model of the Torque and State estimator

The abc to dq transformation in figure 11 is the inverse of the transformation from abc to dq that is a simple linear transformation done by resolving the three vectors into the 2 dimensions d and q, figure 12 represents this transformation, and the analysis of this transformation can be found also in [7].

```
function [Vd,Vq] = fcn(Va,Vb,Vc)
Vd=(2/3)*(Va-(0.5*Vb)-(0.5*Vc));
Vq=(2/3)*(((nthroot(3,2))/2)*Vb-((nthroot(3,2))/2)*Vc);
end
```

Figure. 12. Simulink model of transformation of stator's voltage from abc to dq

```
function [Id,Iq] = fcn(Ia,Ib,Ic)
Id=(2/3)*(Ia-(0.5*Ib)-(0.5*Ic));
Iq=(2/3)*(((nthroot(3,2))/2)*Ib-((nthroot(3,2))/2)*Ic);
end
```

Figure. 12. Simulink model of transformation of stator's current form abc to dq

In addition to that, we are calculating which sector we are in from the 6 sectors given of the voltages' vectors discussed in the SVPWM section, we acquire the value of this vector using this equation [12]:

$$\text{sector number} = \tan^{-1}\left(\frac{\psi_q}{\psi_d}\right)$$

Finally, the estimators block is well-defined and can provide the estimated torque, stator's flux, and the sector where the stator's voltage lies in. So, the remaining part is the controlling brain for deciding actions to the look-up table and the focus of all this project, which is the controller.

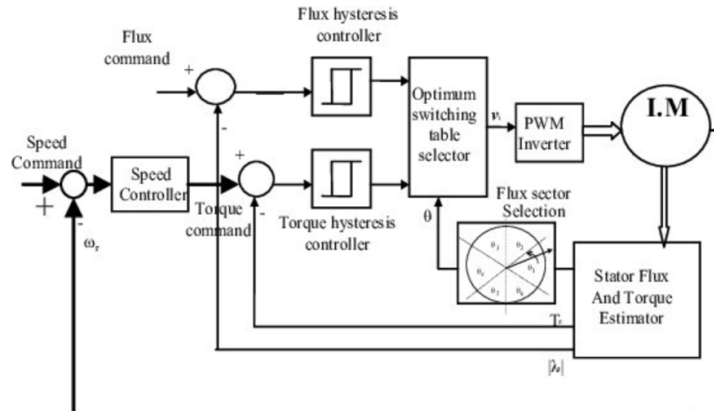
fc	3800
J	0.1390
Ki	35
Kp	8
Llr	0.0156
Lls	0.0156
Lm	0.2848
P	4
Rr	2.4860
Rs	4.1250
ScopeData1	1x1 Dataset
Tlim	15
tout	164567x1 double
Ts	2.0000e-05
Vdc	560
wb	314.1593
Xlr	4.8915
Xls	4.8915
Xm	89.4726
Xml	2.3807

Figure. 14. All parameters of our model

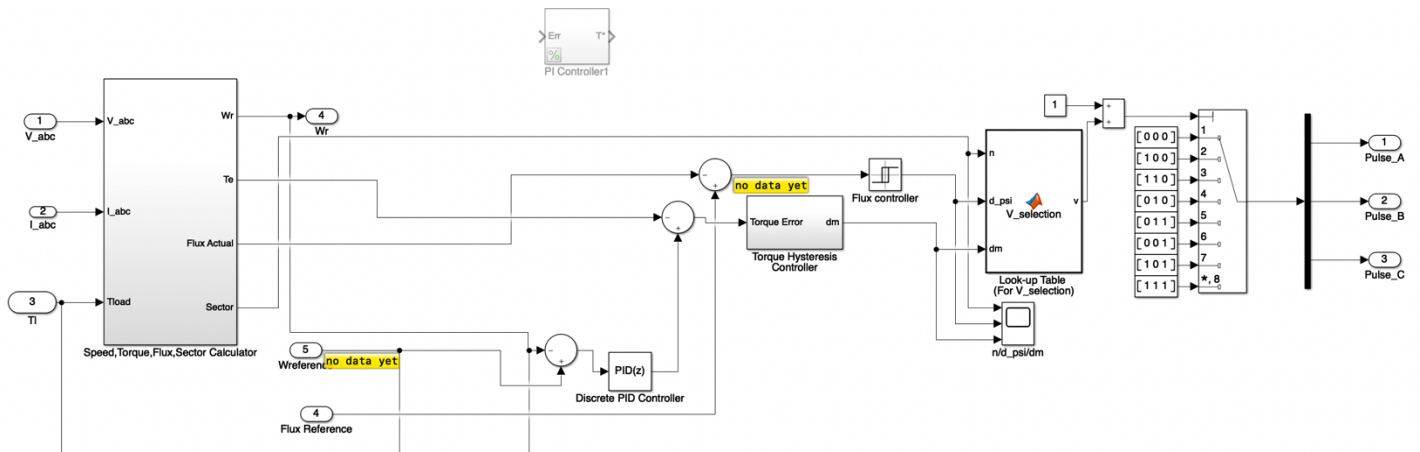
In addition to the given parameters, the model operates at 50 Hz frequency and outputs rated power = 2.2 kw and rated Torque = 14 N.M, that's why it is hard to hold a torque load higher than this.

A) Conventional DTC by PI Controller:

PID is one of the classical controllers that are well-known for their easy implementation and efficiency in non-complex systems. PID is proportional–integral–derivative controller continuously calculates an error value $e(t)$ as the difference between a desired setpoint (SP) and a measured process variable (PV) and applies a correction based on proportional, integral, and derivative terms denoted P, I, and D respectively [13], hence the name. In the conventional DTC, proportional and integral terms are the only used terms.



a) The full control loop of the I.M [14]



b) the PID control of DTC connected to the lookup table to generate signals for the inverters

Figure. 15. PID control of DTC

As shown in figure 15, this is the full loop of controlling Induction motor, which some of its parts are discussed already, like IM, inverter, and switching table. In addition, the hysteresis controllers shown in the figure are just relays to limit the output to a certain range, this will be modified to include flux weakening for controlling above the rated speed. So, here is the well-known PID equation that is used:

$$u(t) = k_p * e(t) + k_i \int e(t)dt + k_d * \frac{de(t)}{dt}$$

A tuned PID controller is utilized to test the performance of our system, we set a stair block to generate different ranges of required speed from 0 to 400 rad/sec in 60 seconds for $T_l = 0, 25, 30$ and 50 N.m.



Figure. 16. The stair block for generating required speed values

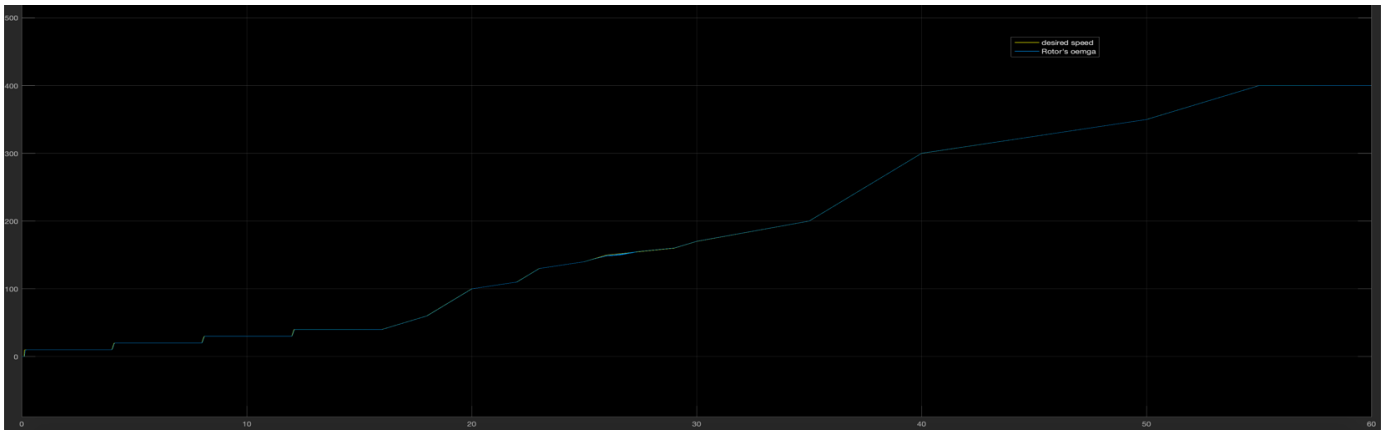


Figure. 17. The error between the desired speed and rotor's speed in case of zero torque load

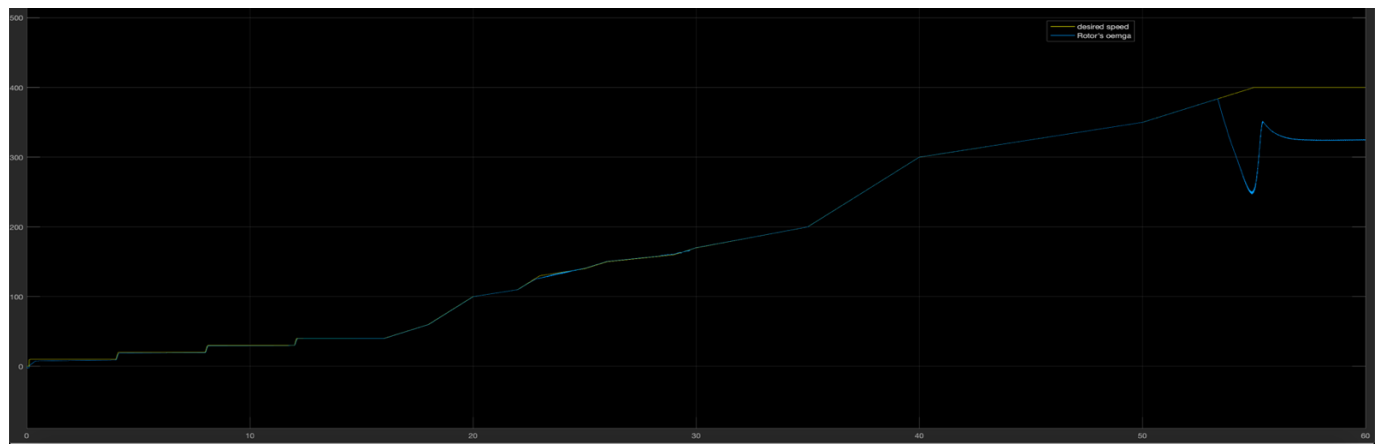


Figure. 18. The error between the desired speed and rotor's speed in case of 25 Nm torque load

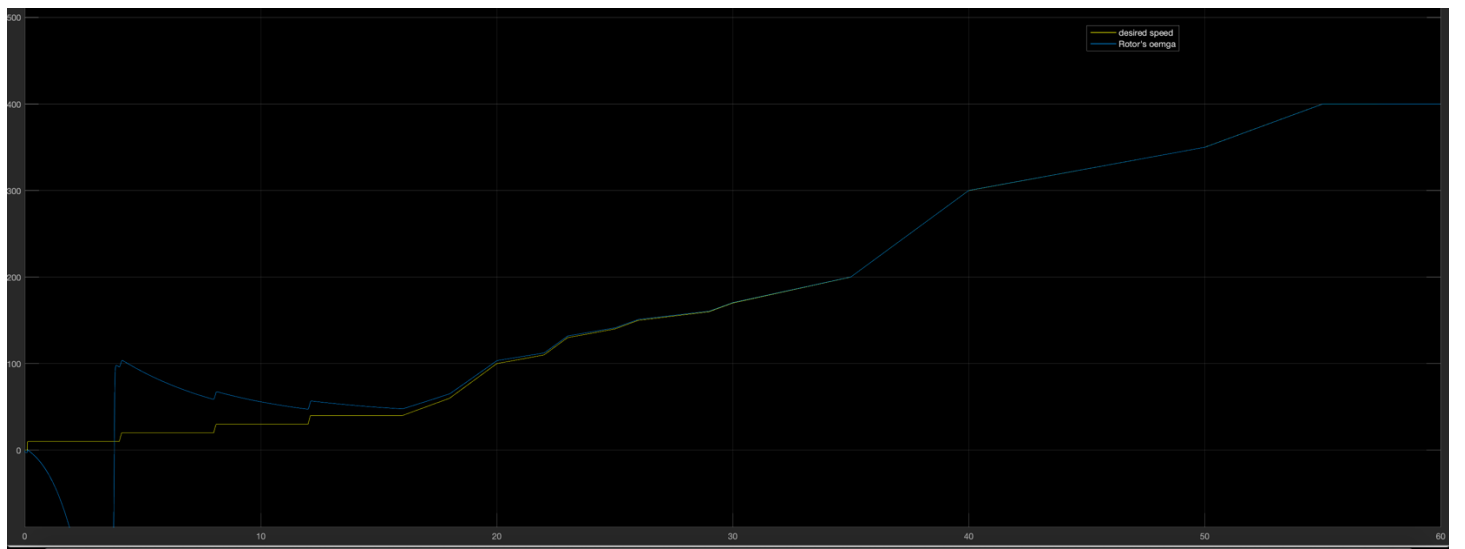


Figure. 19. The error between the desired speed and rotor's speed in case of 30 Nm torque load

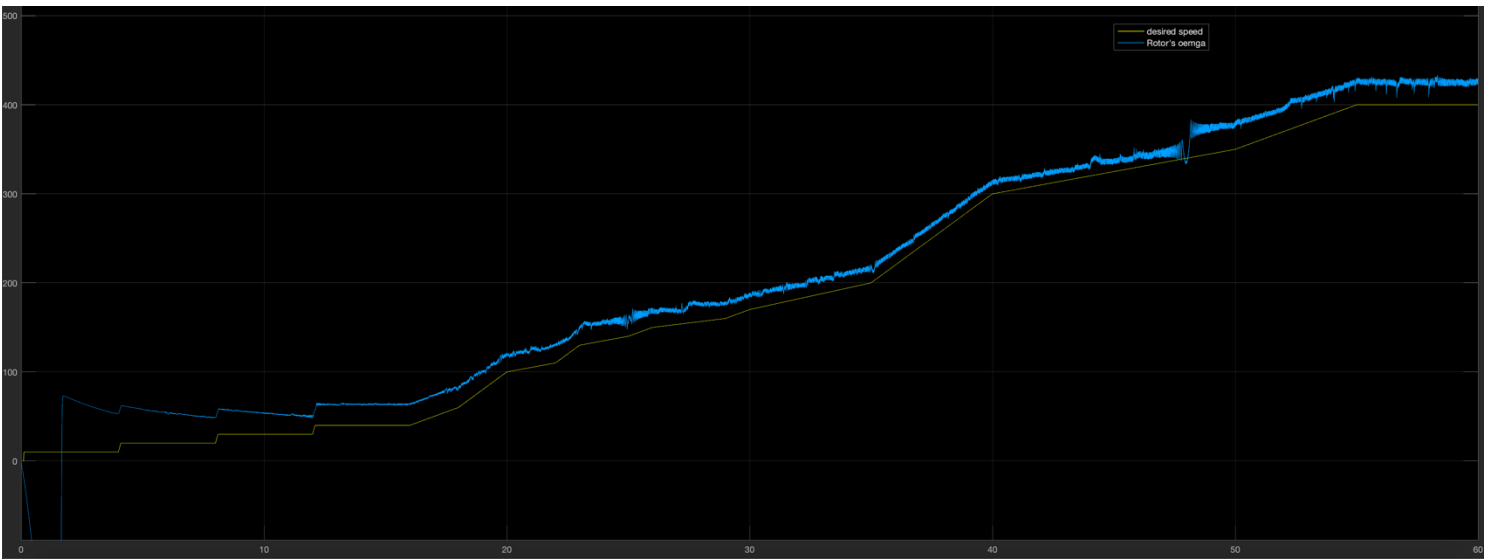


Figure. 20. The error between the desired speed and rotor's speed in case of 50 Nm torque load

After checking all these different cases, it is pretty obvious that in the case of 0 or very low torque loads PID is doing a great job. However, by increasing the torque load to higher values it becomes inefficient, the instantaneous change of speed in the first 10 seconds is because the load torque is higher than the starting torque, as well as the steady state error and the huge noise in the rotor speed that the PID controller is not sufficient enough to handle.

As an example, the torque of the motor for the case of $T_l = 50 \text{ N.m}$:



Figure. 21. The error between the Torque load and the electromagnetic torque produced by the motor

As shown in Figure 21, the torque load at the end is nearly equal to the electromagnetic torque produced by the motor in order to keep rotating with a constant speed, however it was not the required ones. In addition, the huge disturbance in the beginning is very obvious as well, and this is reflected on the speed performance as well as shown in Figure 20.

As a conclusion, the PID control cannot maintain achieving the required speed while resisting a large torque load, it will try to maintain a constant omega but with some fluctuations and with a steady state error, which can be enhanced by some extra assumptions that are not fully practical [13].

The main drawbacks of DTC using PID controllers are the sensitivity of the performances to the system-parameter variations and the inadequate rejection of external disturbances and load changes, as shown in the performance analysis, that's why it is advised to design a more robust control that can handle disturbance and load changes better, as sliding mode control.

B) Enhancement of the performance by utilizing Sliding Mode Control:

The sliding mode control is a nonlinear control method that aims to force the system to "slide" along a defined surface to stabilize robustly, it alters the system dynamics to adapt to these conditions. In addition, it provides an accurate calculation for a good settling time. Although sliding mode has some chattering effects that lead us to use a saturation method to accept a tolerable error, it is one of the powerful controllers that can handle the disturbance of the system and adapt to load changes as we will observe.

The control problem is to get the motor speed a specific time varying command in the presence of model imprecision, load torque disturbances and measurement noise. In sliding mode control, the system is controlled in such a way that the tracking error and its rate of change always move towards a sliding surface. The sliding surface is defined in the state space by the scalar equation [15,16].

$$s(e, \dot{e}, t) = 0$$

Where s is the sliding variable, in this project, two different sliding surfaces will be tested, the linear and integral surfaces, to check their differences. The verification of stability of any sliding mode controller relies on Lyapunov stability analysis using energy approach, that if the energy of any system decays to zero, then this system will stabilize sooner or later [15], this can be validated if the rate of change of the energy of the system is strictly negative.

In this case, the testing will be on a linear surface which is shown by the sliding variable:

$$s = \dot{e} + \lambda e$$

λ is a positive constant that depends on the bandwidth of the system. The problem of tracking is equivalent to remaining on the sliding surface for all the time, and the sliding variable is kept at zero. Control input is applied to drive the system state onto the switching line, and once on it, the system is constrained to remain on the line, however this will cause the chattering problem, so we will determine an acceptable range of error, to remove this chattering phenomenon, also known as low pass filter. The condition of sliding mode is:

$$\frac{1}{2} \frac{d}{dt} s^2 = s \dot{s} \leq -\eta |s|$$

Where η is a positive constant, this equation can be transformed to:

$$sgn(s) \leq -\eta$$

Then, q-axis stator voltage command is responsible for changing torque is:

$$V_{qs}^* = -K \cdot sgn(s)$$

Where K is a positive constant, somehow similar to the k gain in the PID controller explained above, then the chattering activity will be appeared and the sign function could be replaced by saturation function which may give a smoother performance this control input was proposed by El guindy et al. [18]. However, it works for lower load torques only and it did not add a new thing on the PID performance.

As a result, a new sliding surface and analysis is introduced which includes the dynamics of the motor better, so it is expected to perform better than this technique, all the next analysis was done by Aini F. et al [17].

Given that this equation that links the current of the stator in the q frame with the electromagnetic torque of the induction motor:

$$T_e = K_T i_{qs} \quad (2)$$

Where $K_T = \frac{3}{2} \frac{P}{2} \frac{L_m}{L_r} \psi_{dr}$.

The mechanical equation of an induction motor can be written as:

$$T_e = J \dot{w}_m + B w_m + T_L \quad (3)$$

So, merging using (2) into 3, we can obtain:

$$b i_{qs} = \dot{w}_m + a w_m + f$$

Where $a = \frac{B}{J}$, $b = \frac{K_T}{J}$ and $f = \frac{T_L}{J}$

As we are dealing now with the Sliding mode control, we have the privilege of adding uncertainties as Δa , Δb and Δf in term a, b and f respectively, as follows:

$$\dot{w}_m = -(a + \Delta a)w - (f + \Delta f) + (b + \Delta b)i_{qs}$$

The tracking speed error is defined as

$$e(t) = w_m(t) - w_m^*(t)$$

where w_m^* is a rotor speed reference. Taking derivative of previous equation with respect to time yields:

$$\dot{e}(t) = \dot{w}_m(t) - \dot{w}_m^*(t) = -ae(t) + u(t) + d(t)$$

Where,

$$u(t) = bi_{qs} - aw_m^*(t) - f(t) - \dot{w}_m^*(t)$$

And the uncertainties $d(t)$

$$d(t) = -\Delta aw_m(t) - \Delta f(t) + \Delta bi_{qs}$$

Now, the sliding variable $S(t)$ will be defined with an integral surface and not a linear one, which is expected to perform better in our model.

$$S(t) = e(t) - \int_0^t (k - a)e(\tau)d\tau$$

Where k is a constant gain. When the sliding mode occurs on the sliding surface, then $S(t) = \dot{S}(t) = 0$ and therefore the dynamical behavior of the controlled system can be expressed as:

$$\dot{e}(t) = (k - a)e(t)$$

In order to obtain the speed trajectory tracking, the following assumption has been formulated in [18]

Assumption 1: The k must be chosen so that the term $(k - a)$ is strictly negative and hence $k < 0$, therefore the sliding surface is defined as:

$$S(t) = e(t) - \int_0^t (k - a)e(\tau)d(\tau) = 0$$

The variable structure controller is design as:

$$u(t) = ke(t) - \beta sgn(S)$$

Where β is a switching gain, S is the sliding variable and $sgn(.)$ is the sign function defined as:

$$sgn(S(t)) = \begin{cases} 1 & \text{if } S(t) > 0 \\ -1 & \text{if } S(t) < 0 \end{cases}$$

Assumption 2: the gain β must be chosen so that $\beta \geq |d(t)|$ all the time.

When sliding mode occurs on the sliding surface, then $S(t) = \dot{S}(t) = 0$ and the tracking error converges to zero exponentially. From (23) and (28), the current command i^*_{qs} can be obtained as:

$$i^*_{qs} = \frac{1}{b} [ke - \beta sgn(S) + aw_m^*(t) + \dot{w}_m^*(t) + f]$$

However, in our model, our required output should be Torque and not i^*_{qs} , so we substitute this equation in (2), the torque output of the SMC controller will be equal to:

$$T_e = J * [ke - \beta sgn(S) + aw_m^*(t) + \dot{w}_m^*(t) + f]$$

Therefore, the above design sliding mode speed controller resolves the speed tracking problem under parameters uncertainty and load disturbances. By using Lyapunov function candidate, the proof of this theorem is deduced, this function is chosen as it is positive definite function for all its domain, this is the first rule of Lyapunov function.

$$V(t) = 0.5S(t)^2$$

The first derivative of this equation, for Lyapunov stability analysis check, is:

$$\dot{V}(t) = S(t)\dot{S}(t) = S(t)[\dot{e}(t) - (k - a)e(t)]$$

Substituting in the first derivative of the Lyapunov function,

$$\begin{aligned}\dot{V}(t) &= S(t)[- \beta \operatorname{sgn}(S) + d(t)] \\ &= -\beta |S(t)| + d(t)S(t) \\ &\leq -\beta |S(t)| + |d(t)||S(t)| \\ &\leq -[\beta - |d(t)|] |S(t)| \leq 0\end{aligned}$$

Using the second assumption, then the first derivative of Lyapunov function is not positive, then the sliding mode reaching condition is satisfied, and the stability of this controller is achieved.

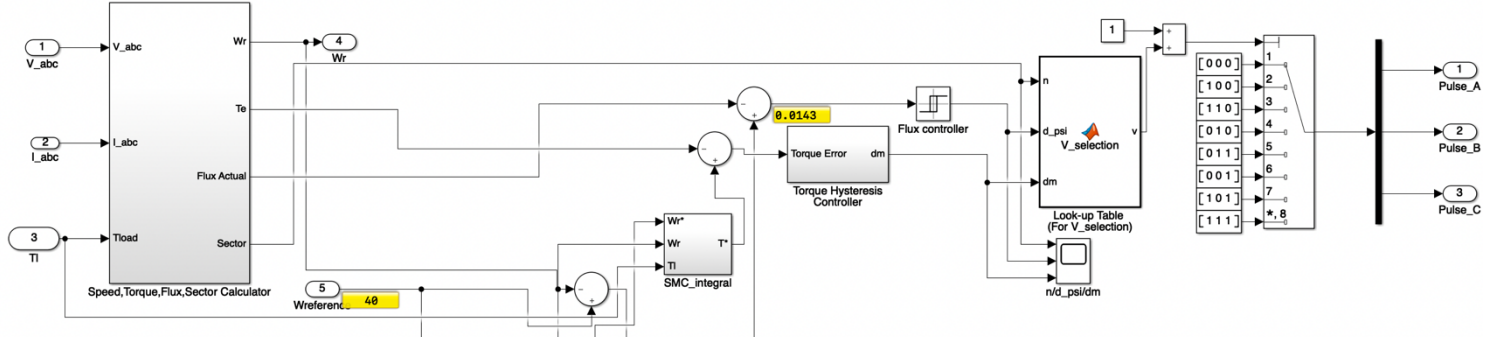


Figure. 22. The SMC control is inserted instead of the PID

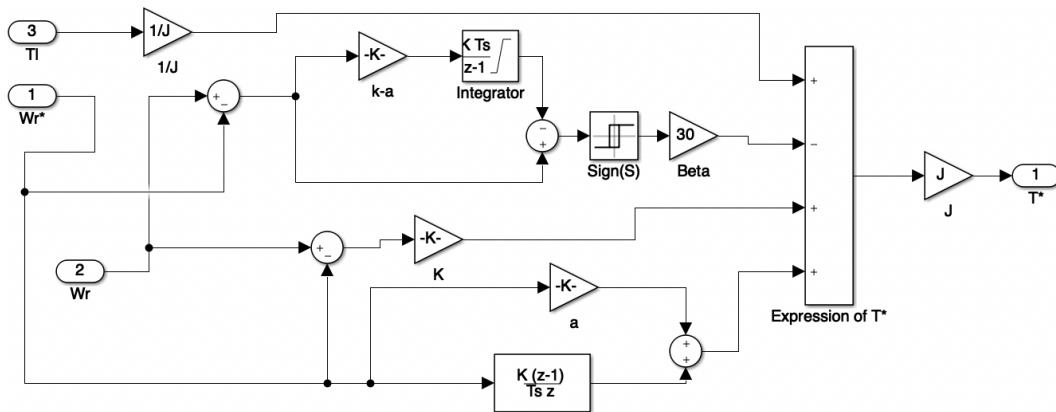


Figure. 23. The SMC control block equation shown here,

The K and β gains are assumed to be -1000 and 30 respectively to satisfy the assumptions made in the derivations. After that, this control method will be tested for the same test cases of the PID control but with addition of extra friction component.

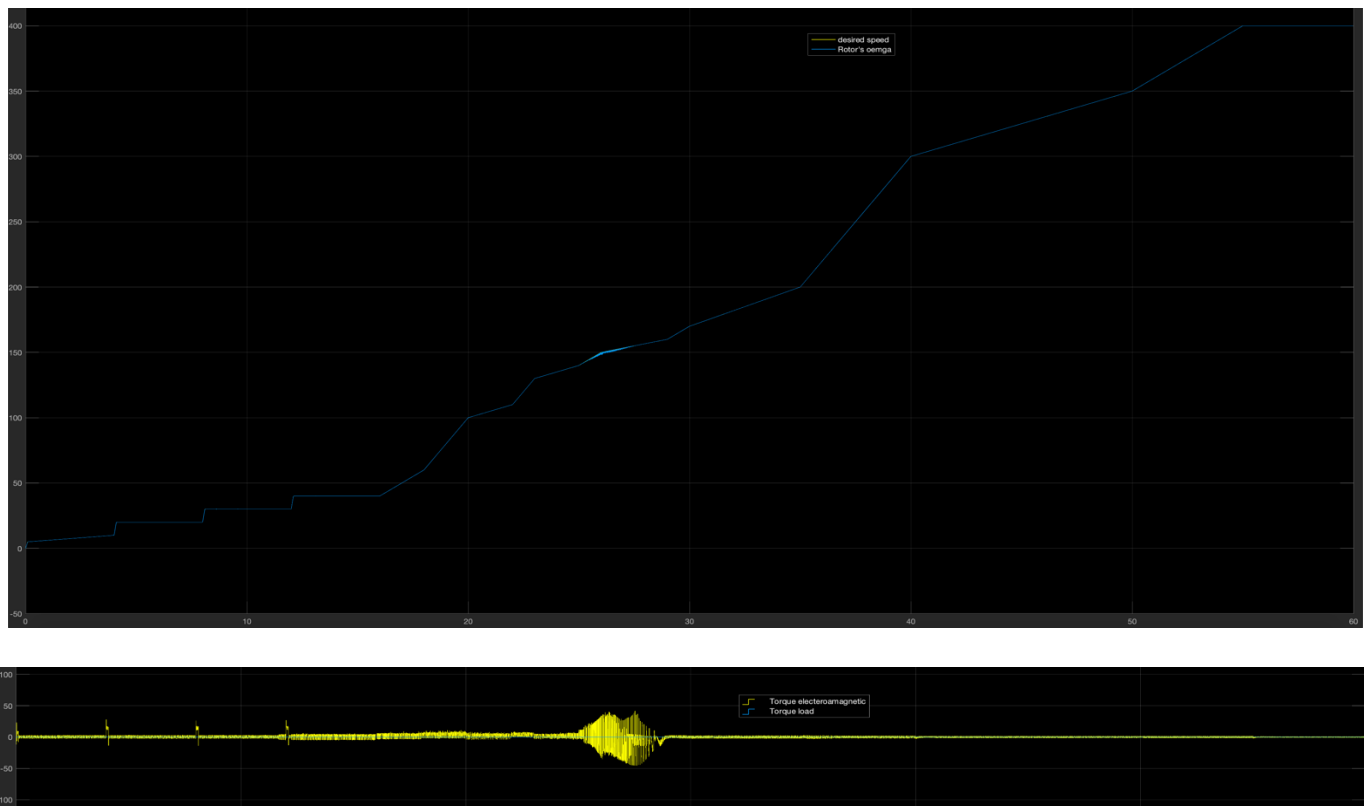


Figure. 24. The error between the desired speed and rotor's speed in case of zero torque load

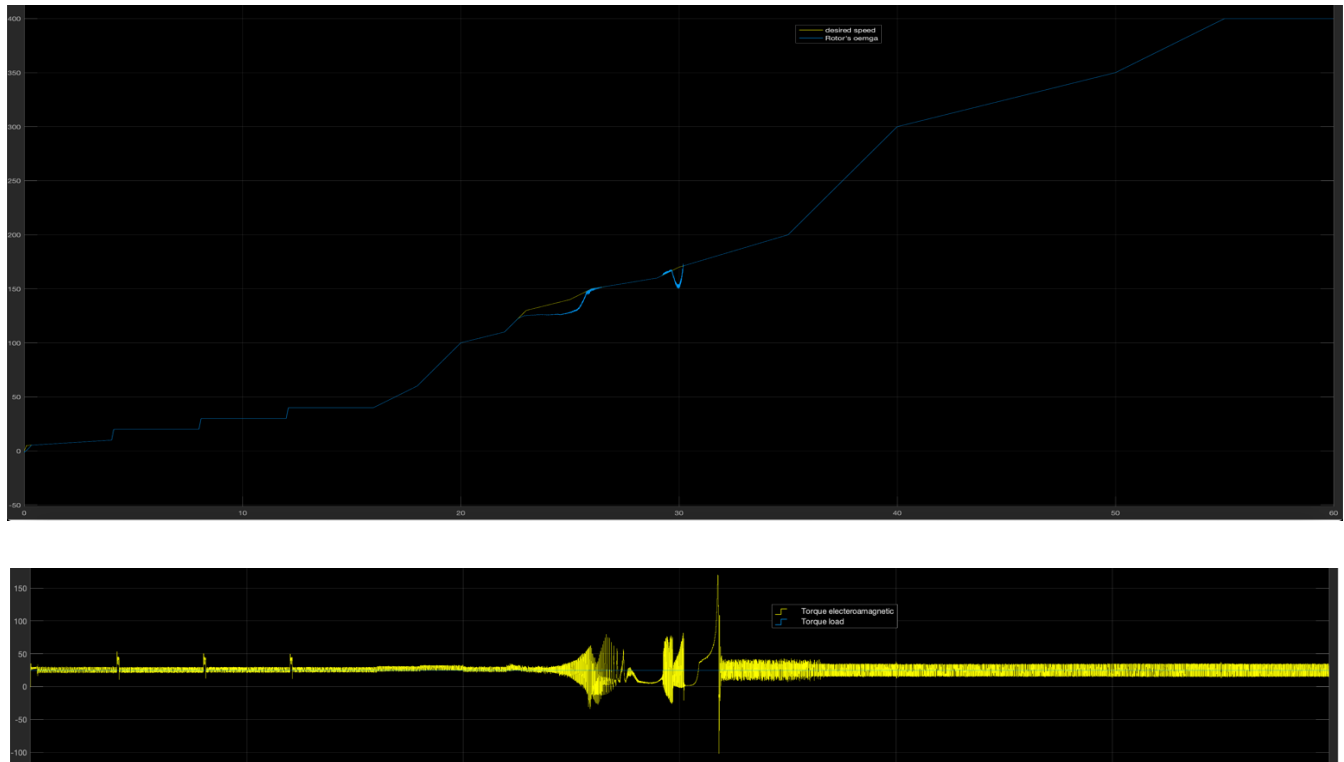


Figure. 25. The error between the desired speed and rotor's speed in case of 25 Nm torque load

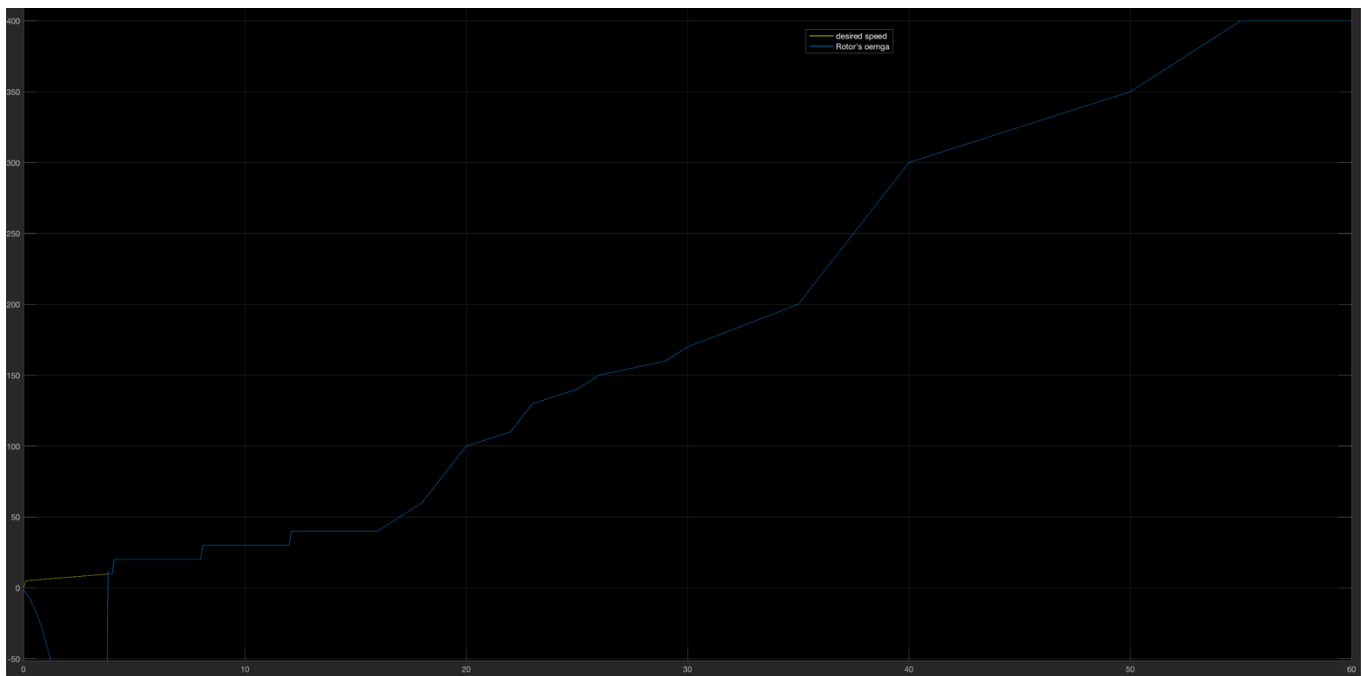


Figure. 26. The error between the desired speed and rotor's speed in case of 30 Nm torque load

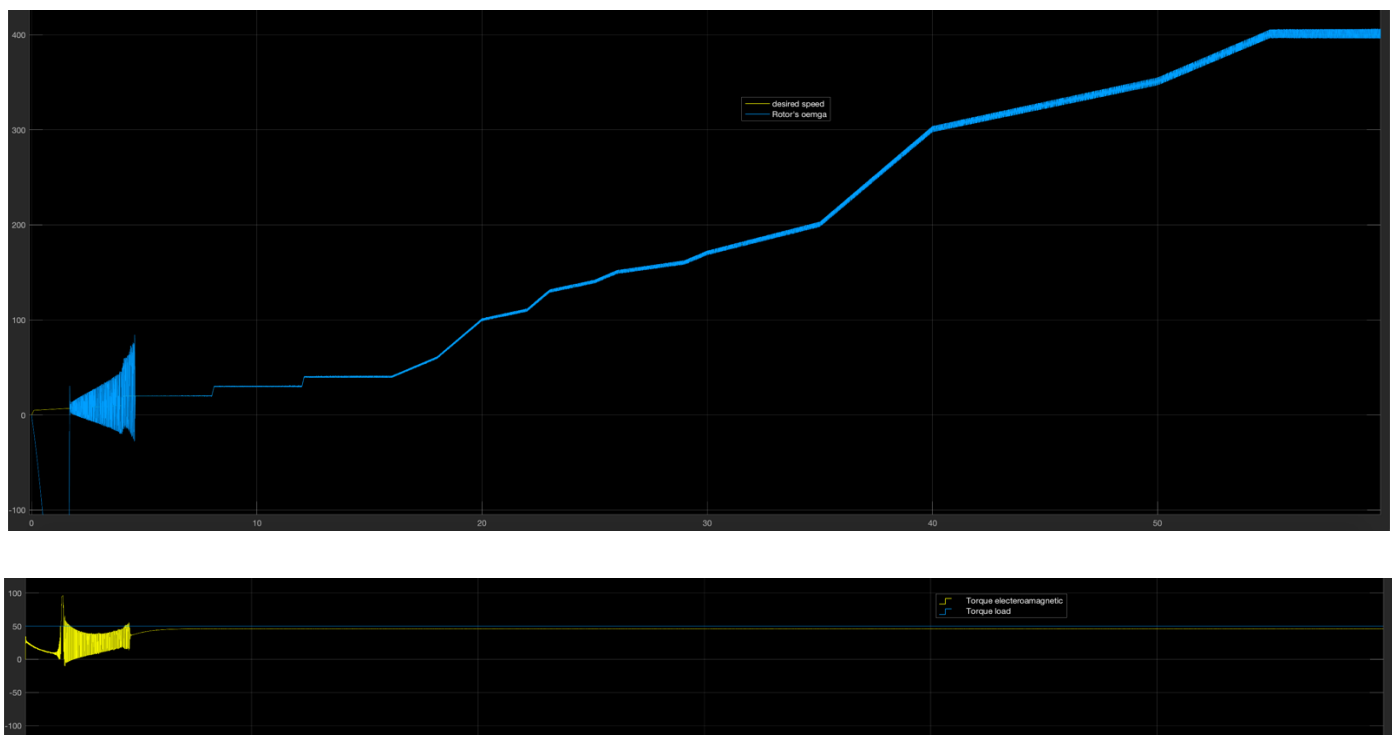


Figure. 27. The error between the desired speed and rotor's speed in case of 50 Nm torque load

By observing the differences between the SMC response regarding the adding of extra friction as well to make the mission of this controller harder, but its robustness and adaptation to any errors is strong enough to handle the different required speed even if the torque load is very high like 50 N.m. However, in the case of high torque loads, a starting disturbance is occurred because the torque load becomes greater than the starting torque which takes time from the controller to adapt to this load until the SMC is successfully controls all the different speeds as shown in the figures.

The next simulations show the actual robustness of the SMC, where a sine wave disturbance is added as shown:

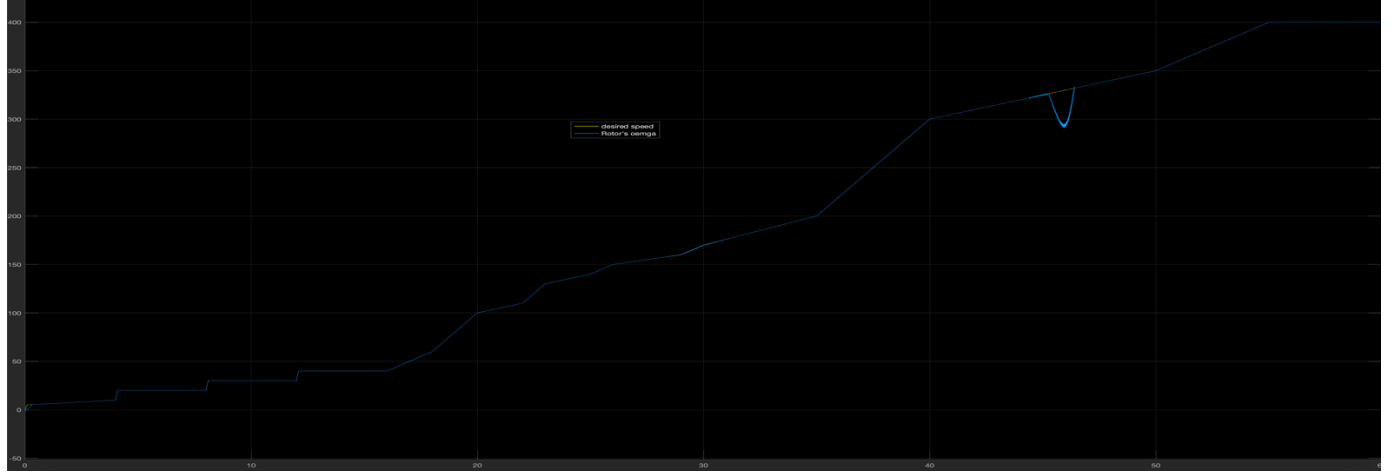


Figure. 29. The error between the desired speed and rotor's speed, in case of 25 Nm torque load and added disturbance of sine wave with amplitude 25

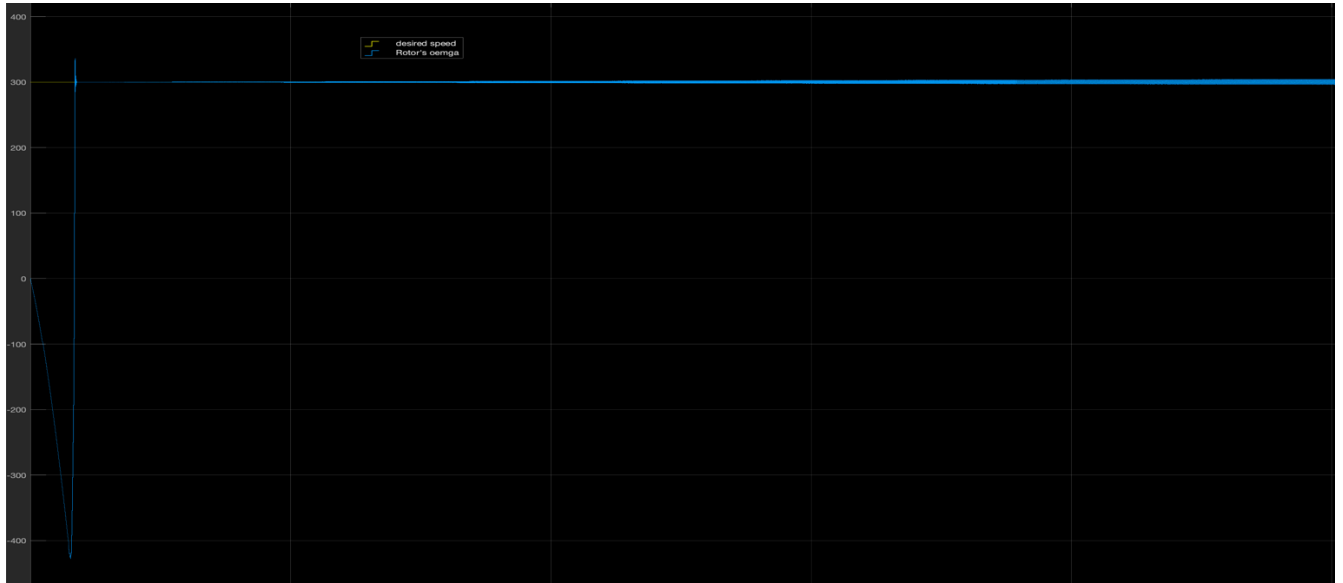


Figure. 29. The error between achieving 300 rad/sec and rotor's speed, in case of 50 Nm torque load and added disturbance of sine wave with amplitude 25

In Figure 29, it is very obvious that the SMC did its job very well, the PID failed to achieve any given speed in case of a high load like 50 N.M. The SMC did also work very well in the presence of such a disturbance, that is why it is very well-designed for this purpose.

A sliding mode control with integral sliding surface for high performance induction motor has been developed for this project. Using a simple field weakening, it is ensure to control torque and flux separately for the purpose of DTC.

C) Control Using Constant Volt/Frequency:

V/f Control is the most popular technique and has found wide range of applications in industrial and domestic area's due its ease-of-implementation.[20]. The basic theory behind constant V/Fcontrol relies on the concept of maintaining proportionality between the relation of $V1 \propto \Phi f$ where $V1$ is the Voltage, f is the frequency and Φ is the air-gap flux. Therefore, if we want to reduce the frequency, we have to reduce the voltage also, otherwise the air-gap flux will provide distortion to the stator flux which is undesirable. Therefore, whenever frequency is changed to control a new speed, the terminal voltage is also changed to maintain the V/f ratio constant.[20]

The following is an example of a model of the V/F control technique of induction motor using SVPWM. It can be dissected into three components. The First Component is the three-phase inverter with SVPWM generator. The second component is the three-phase asynchronous induction machine used. The third component is the V/F control loop [19].

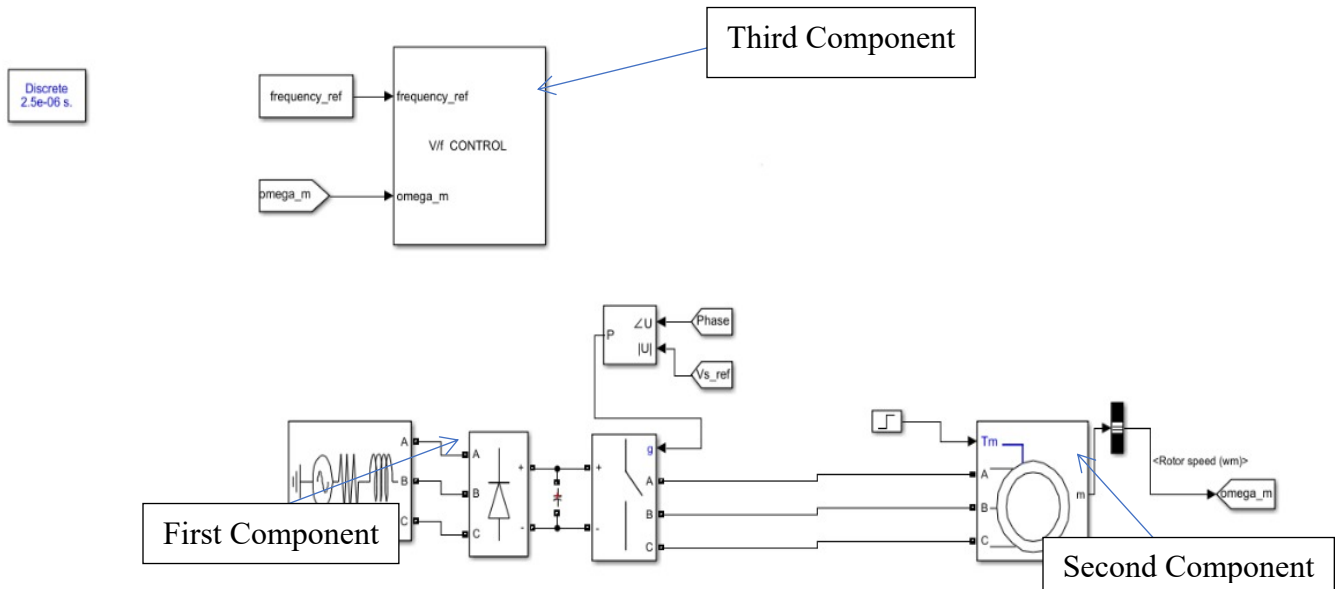
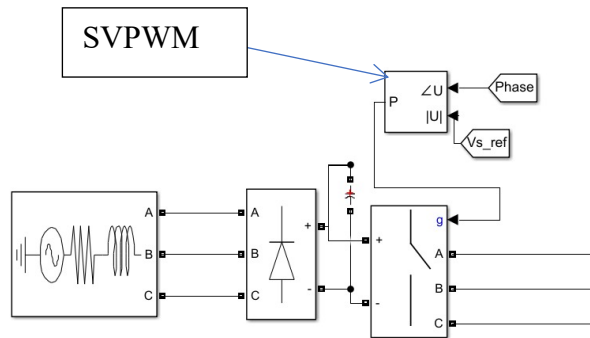


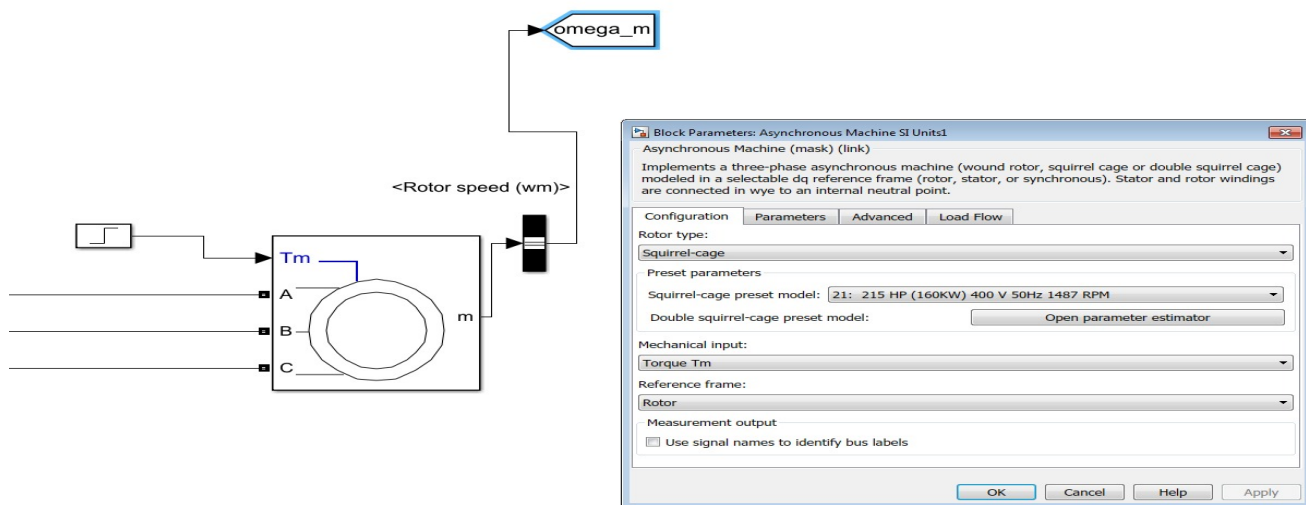
Figure. 30. The full picture of the V/F control loop and explaining each component in the following sub-figures

The First component:



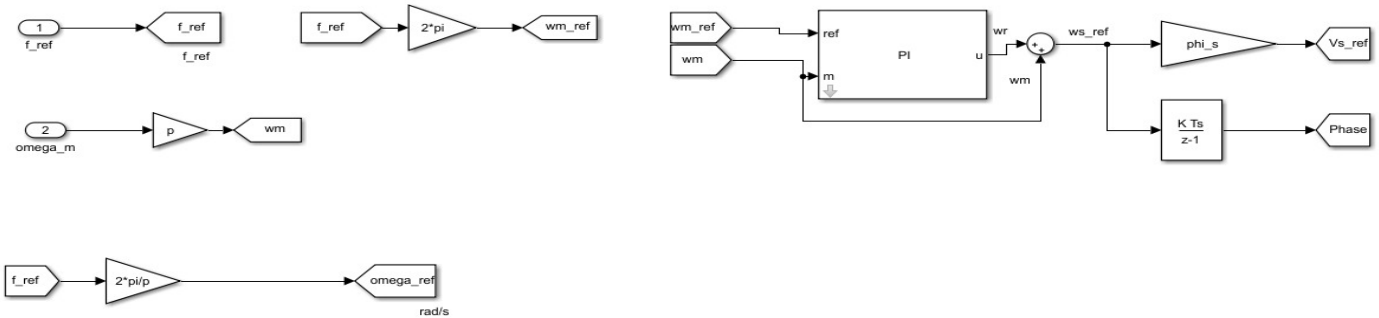
- Three Phase Source YG Configuration 490 RMS Hz 50.
- Arm Bridge with Diode as the power electronic Device.
- Arm Bridge with Switches as the power electronic Device.
- Built in SVPWM to generate the pulses required to operate the switches which takes the Voltage stator reference and the phase angle as inputs.

The second Component:



A Squirrel Cage Model rotor type is chosen with a preset model as shown in the following figure.

The third Component:



This is the control loop implemented Where the speed error is controlled by a PI controller and then added to the omega motor to achieve w_{s_ref} . Then it's multiplied by gain to achieve V_{s_ref} and also w_{s_ref} is integrated to achieve the stator phase. These Variables Voltage and Phase respectively as mentioned before generate the pulses for the three-phase inverter when passed by SVPWM(Space Vector Pulse Width Modulation).

Results:

The following test case is done by generating a frequency step as shown in the figure below and then multiplying it by 2π to get the desired omega reference. The results can be shown in the figure below:

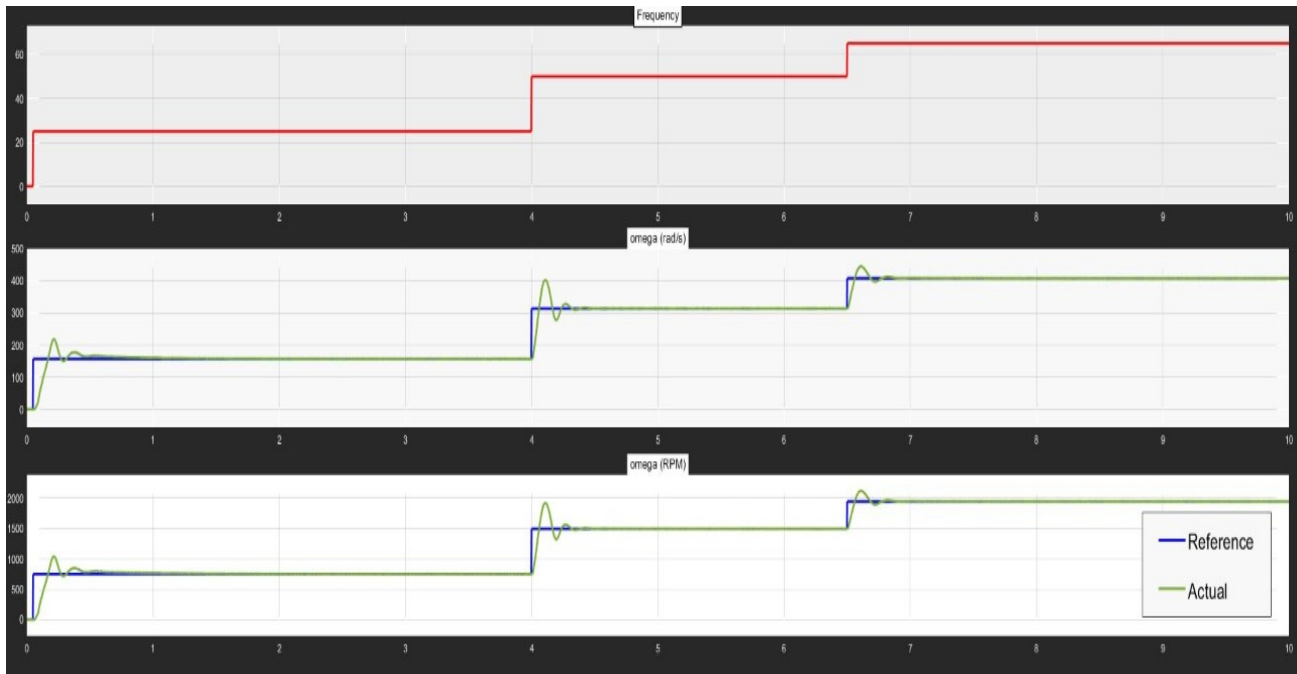


Figure. 31. The frequency output, angular speed and rotor speed with torque load of 2Nm, KP 0.17 and KI 0.3288

It can be observed that the V/F technique with a PI controller is able to track the desired reference with good performance and a slight overshoot can only be observed when the speed suddenly increases. However, this can be removed by gradually increase the speed linearly, therefore removing the step response effect.

The following figure is the response of stator flux, voltage ref and frequency stator, this graph is done in order to visualize and verify that a relation between V/F and the stator flux:

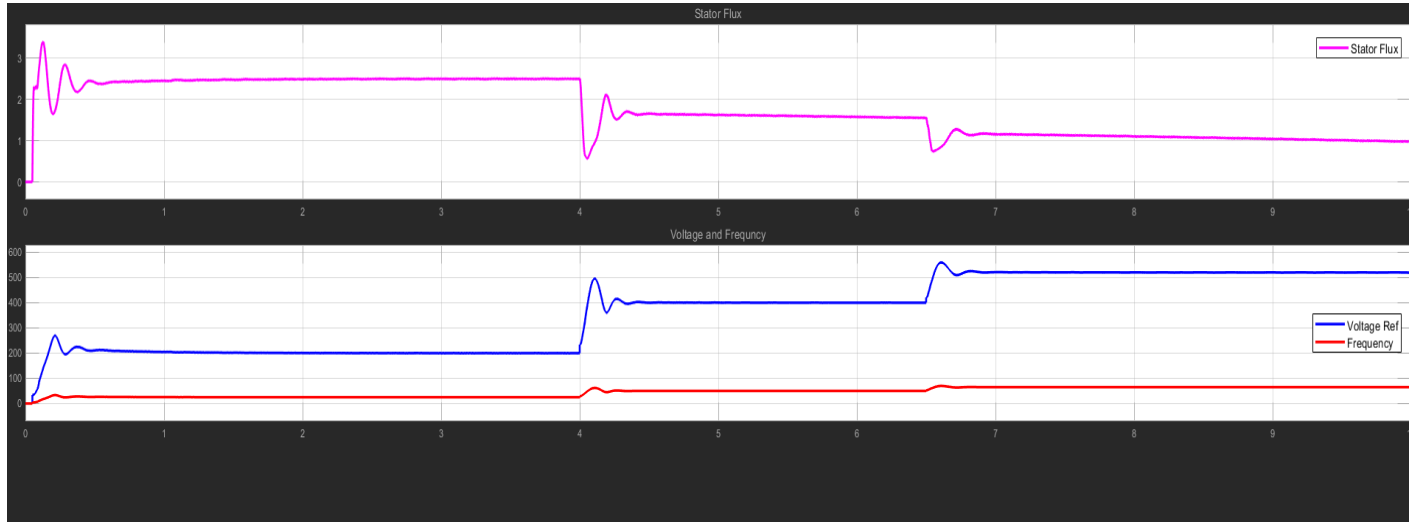


Figure. 32. The Stator Flux, Voltage and Frequency with torque load of 2Nm, KP 0.17 and KI 0.3288

It can be observed from time 0 to 0.7 sec that when the frequency increases the voltage also increase to maintain the ratio and finally achieve a constant flux during an interval from 0.7 till 4. At time 4 we are increasing the speed, therefore we want to decrease the flux and increase again the voltage and frequency to keep the flux constant however at a lower value.

A test case will be performed with a linear reference omega with slope of 10 and final value at 100 to remove sudden rises. The results were as follows:

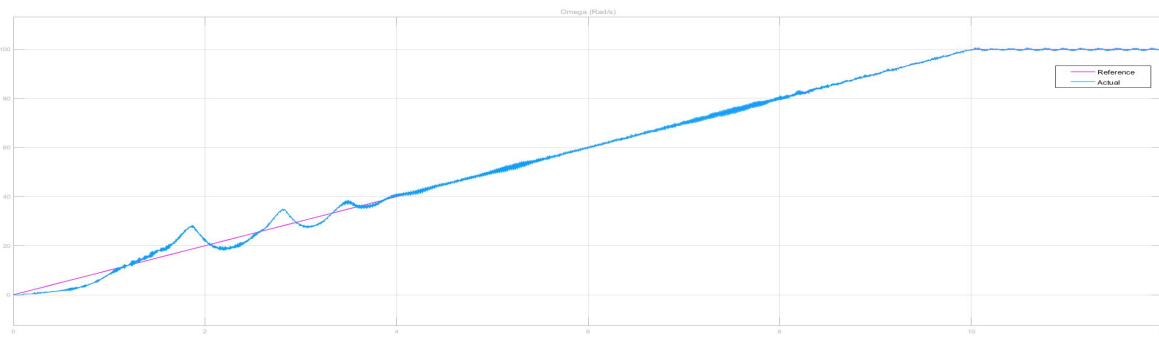


Figure. 33. Angular with torque load of 2Nm, KP 0.2 and KI 0.5

The results show that during the first 4 sec the controller had difficulty in reaching the reference. However, after the 4 sec mark the controller is able to track the desired reference with no overshoot. In order to adjust the early part, we need to adjust the controller gains KP and KI. To do so we can apply the trial and error method to obtain the gains as shown in the following figure.

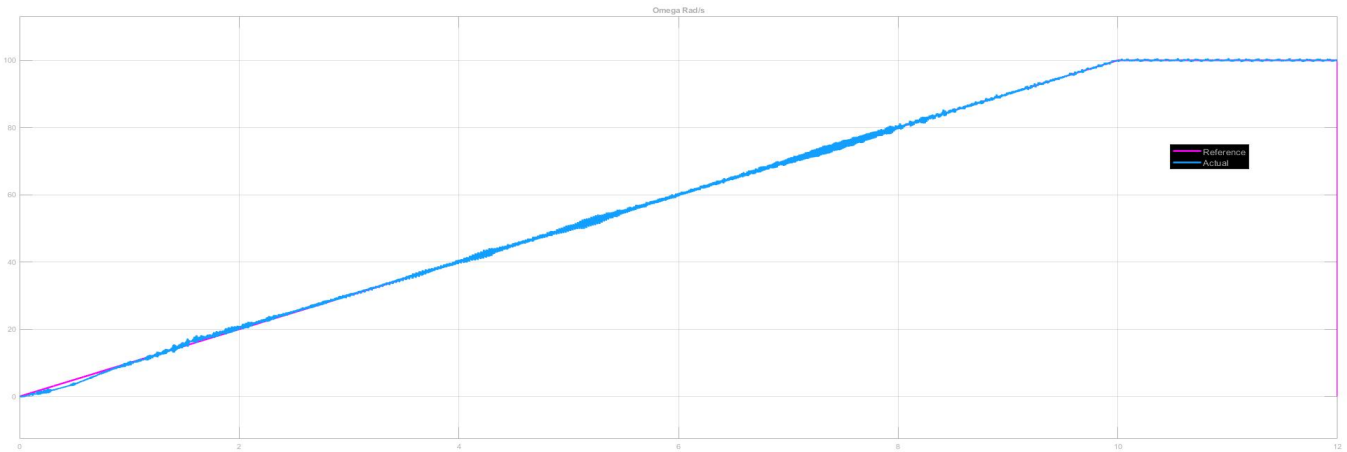


Figure. 34. Angular with torque load of 2Nm, KP 1 and KI 1

The results show that the controller is now able to track the desired reference in all stages due to adjusting the gains of KP and KI to 1. A few other tests were also performed at higher gains. However, the performance results weren't satisfactory.

A V/F technique with PI controller was used to test performance of induction motor. It was able to track the desired reference with good performance after adjusting the gains.

6. Conclusion and future work recommendations:

In conclusion, there are a lot of methods and research contributed in accurate controlling for the induction motor, that's because its wide utilization in many of the applications. Direct Torque Control (DTC) is a very good method for induction motor, and it has a lot of applications. However, the choice of the method of control is an important task. As shown in the above sections, a non-linear controller as sliding mode control is more robust and can handle disturbances better than a classical controller like PID. That differences in performance returns back to the Torque-speed characteristics of the 3 Phase induction motor, which is a non-linear relation, as shown in figure 35. This non-linear relation requires implementing a non-linear controller to avoid messing with any un-modeled dynamics as well as the problems of linearization for any system.

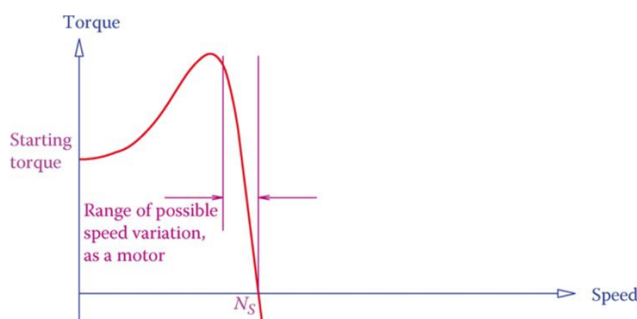


Figure 35. Torque-speed characteristic curve of a three-phase induction motor

As a recommendation for future work, it is advisable to try to fix the challenges faced with the results obtained from the merging of DTC and V/F technique when trying to duplicate the same results as PI and V/F. (Simulink work done will be presented in the appendix). In addition to that, there is also indirect and direct Field Oriented Control (FOC), that has gained a lot of attention for research and applications that is useful as experimented in some papers.

In order to solve the problem of better disturbance rejection, noise sensitivity and achieve a good dynamic performance. A robust and optimal controller as H-infinity can be used. It uses a selection of the weighting functions based on performance requirements to design a controller that is able to achieve the robustness and performance goals required. This enables the motor to work in a wider range of operating conditions [21].

In order to achieve better performance, speed tracking or quick dynamic response, Model Predictive Control (MPC) can be used. It's an optimal controller which solves an optimal control problem (OCP) to obtain the optimal control action needed to drive the model to a required goal. According to [22], it is a powerful alternative to the FOC or DTC in high performance situations. This is due to the capability of eliminating the standard use of switching tables to obtain voltages and use as mentioned above a cost function or an OCP to be minimized to achieve the optimal voltages (Optimal control action) while under a certain set of constraints that are obtained based on the desired performance.

In addition, Fuzzy Logic Control can be used to enhance the performance of the DTC and to minimize the torque ripple problem by varying the duty ratio of the selected voltage vector during each switching period according to the magnitude of the torque error and position of the stator flux [24].

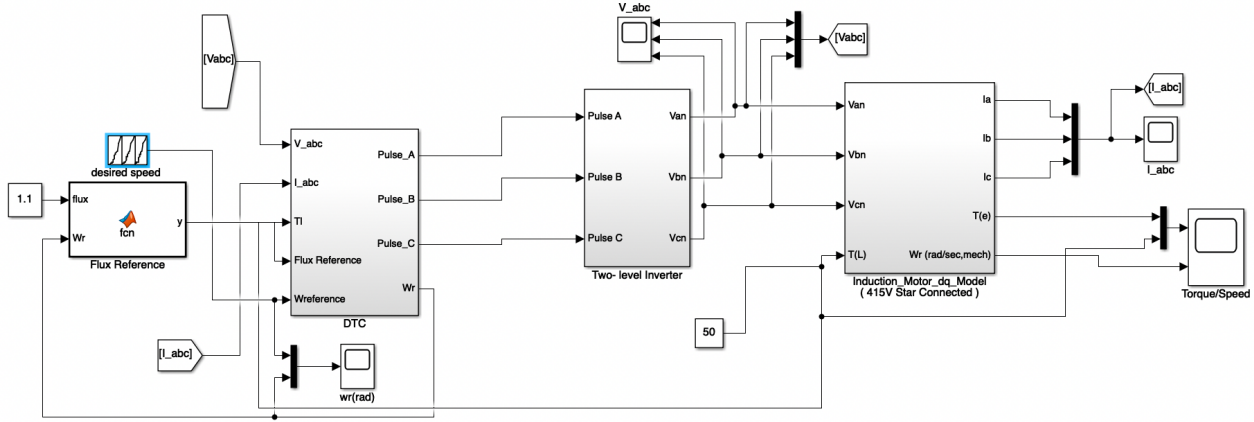
References:

- [1] Rajashekara, Kaushik, Atsuo Kawamura, and Kouki Matsuse, eds. Sensorless control of AC motor drives: speed and position sensorless operation. New York: IEEE press, 1996.
- [2] Blaschke, Felix. "The principle of field orientation as applied to the new transvector closed-loop system for rotating-field machines." Siemens review 34.3 (1972): 217-220.
- [3] Takahashi, Isao, and Toshihiko Noguchi. "A new quick-response and high-efficiency control strategy of an induction motor." IEEE Transactions on Industry applications 5 (1986): 820-827.
- [4] Depenbrock, M. "Direct Self Control of Inverter-Fed Induction Machines 'IEEE Trans. on Power Electronics, Vol.'" (1988): 420-429.
- [5] Tiitinen, Pekka, Pasi Pohjalainen, and Jarkko Lalu. "The next generation motor control method: Direct torque control (DTC)." EPE Journal 5.1 (1995): 14-18.
- [6] Alnasir, Z. A., and A. H. Almarhoon. "Design of direct torque controller of induction motor (DTC)." International Journal of Engineering and Technology (IJET) 4.2 (2012): 54-70.
- [7] Marino, R., Tomei, P, and Verrelli, C., "Induction motor control design", Textbook © Springer-Verlag London limited, 2010.
- [8] Arulmozhiyal, R., and K. Baskaran. "Space Vector Pulse Width Modulation Based Speed Control of Induction Motor using Fuzzy PI Controller." International Journal of Computer and Electrical Engineering 1.1 (2009): 98.
- [9] Mondal, S.K.; Bose, B.K.; Oleschuk, V.; Pinto, J.O.P, "Space vector pulse width modulation of three-level inverter extending operation into overmodulation region", IEEE Transactions on Power Electronics Volume 18, Issue 2, March 2003 Page(s):604 – 611.
- [10] Iqbal, Atif, Adoum Lamine, and Imtiaz Ashraf. "Matlab/Simulink model of space vector PWM for three-phase voltage source inverter." Proceedings of the 41st International Universities Power Engineering Conference. Vol. 3. IEEE, 2006.
- [11] Bojoi, Radu, et al. "Direct torque control for dual three-phase induction motor drives." IEEE Transactions on Industry Applications 41.6 (2005): 1627-1636.
- [12] Pimkumwong, Narongrit, Amorn Onkrong, and Tirasak Sapaklom. "Modeling and simulation of direct torque control induction motor drives via constant volt/hertz technique." Procedia Engineering 31 (2012): 1211-1216.

- [13] Ang, Kiam Heong, Gregory Chong, and Yun Li. "PID control system analysis, design, and technology." *IEEE transactions on control systems technology* 13.4 (2005): 559-576.
- [14] Gadoue, Shady M., D. Giaouris, and J. W. Finch. "Tuning of PI speed controller in DTC of induction motor based on genetic algorithms and fuzzy logic schemes." *Proceedings of the 5th International Conference on Technology and Automation*. 2005.
- [15] Young, K. David, Vadim I. Utkin, and Umit Ozguner. "A control engineer's guide to sliding mode control." *IEEE transactions on control systems technology* 7.3 (1999): 328-342.
- [16] El-Gendy, Eman, et al. "A sliding mode controller for a three phase induction motor." *International Journal of Computer Applications* 64.11 (2013).
- [17] Patakor, Fizatul Aini, Marizan Sulaiman, and Zulkifilie Ibrahim. "Performance of sliding mode control for three phase induction motor." *2010 International Conference on Science and Social Research (CSSR 2010)*. IEEE, 2010.
- [18] Barambones, Oscar, et al. "An adaptive sliding mode control scheme for induction motor drives." *International Journal of circuits, systems and signal processing* 1.1 (2007): 73-78.
- [19] El-Saady, G., Ibrahim, E. N. A., & Elbesealy, M. (2013). V/f control of three phase induction motor drive with different PWM techniques. *Innovative Systems Design and Engineering*, 4(14), 131-144.
- [20] Jee, Devraj, and Nikhar Patel. V/f control of induction motor drive. Diss. 2013.
- [21] Diab, Ahmed A. Zaki, et al. "Robust speed controller design using Hinfinity theory for high-performance sensorless induction motor drives." *Energies* 12.5 (2019): 961.
- [22] Zhang, Yongchang, Bo Xia, Haitao Yang, and Jose Rodriguez. "Overview of model predictive control for induction motor drives." *Chinese Journal of Electrical Engineering* 2, no. 1 (2016): 62-76.
- [23] Pimkumwong, N., Onkrong, A., & Sapaklom, T. (2012). Modeling and simulation of direct torque control induction motor drives via constant volt/hertz technique. *Procedia Engineering*, 31, 1211-1216.
- [24] Hagh, H. V., Eskandari, B., Pashajavid, E., & Bina, M. T. (2011, February). An experimental examination of a fuzzy logic-based DTC scheme. In *2011 2nd Power Electronics, Drive Systems and Technologies Conference* (pp. 251-255). IEEE.

Appendix:

Full diagram of the DTC main blocks:



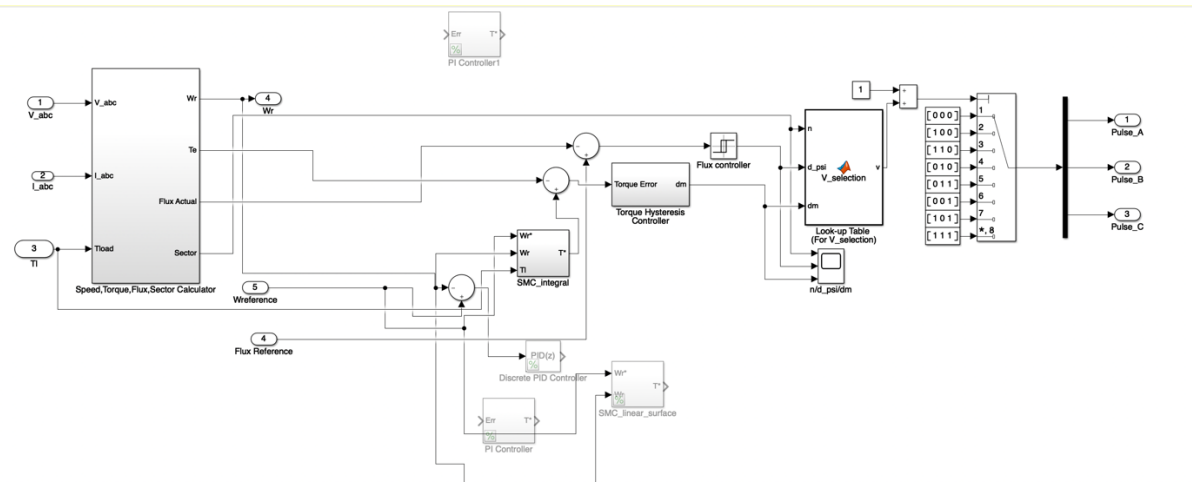
Flux reference block (field weakening):

```

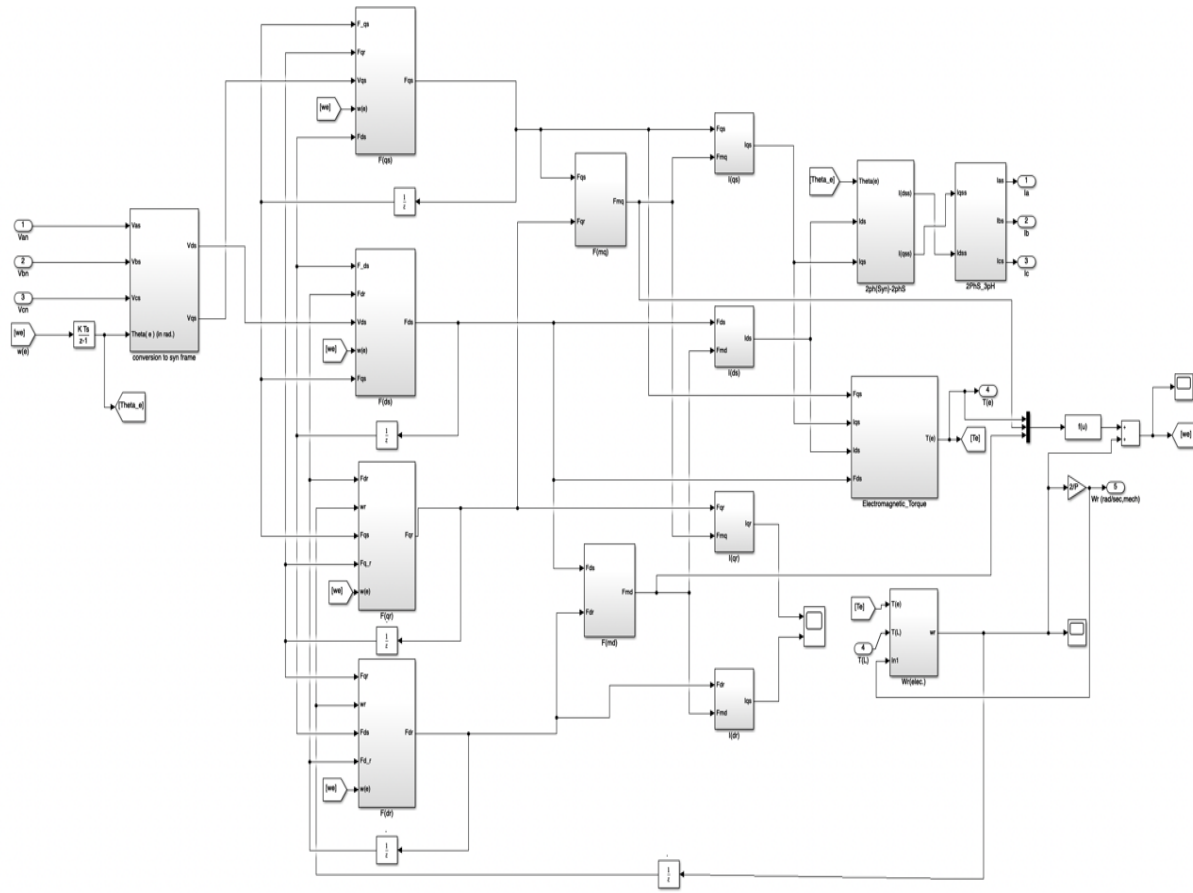
function y = fcn(flux,Wr)
Wbase = 314.1593;
if Wr>Wbase
    y = flux*(Wbase/Wr);
else
    y = flux;
end

```

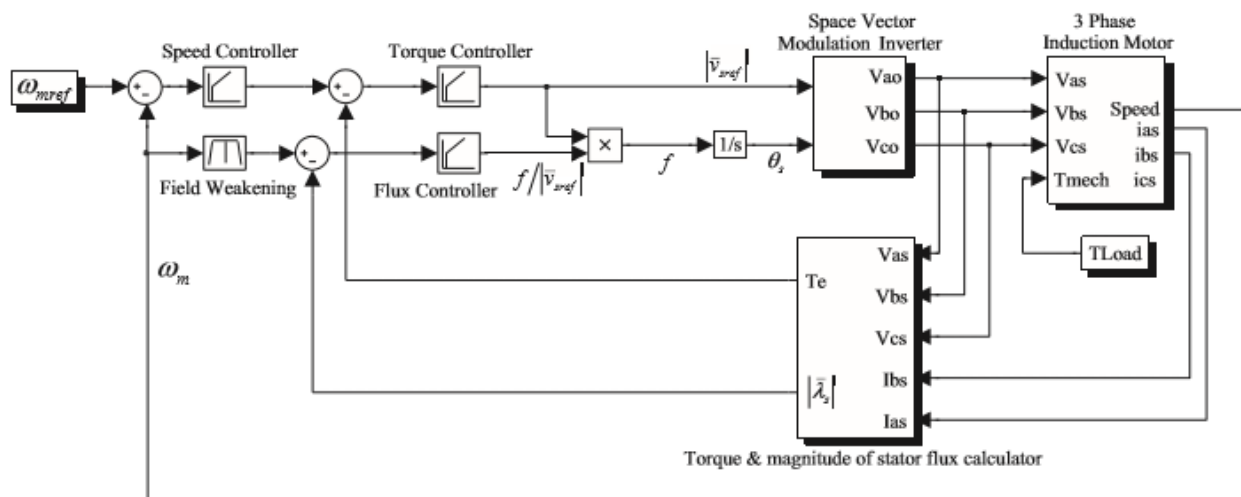
Full image of DTC control:



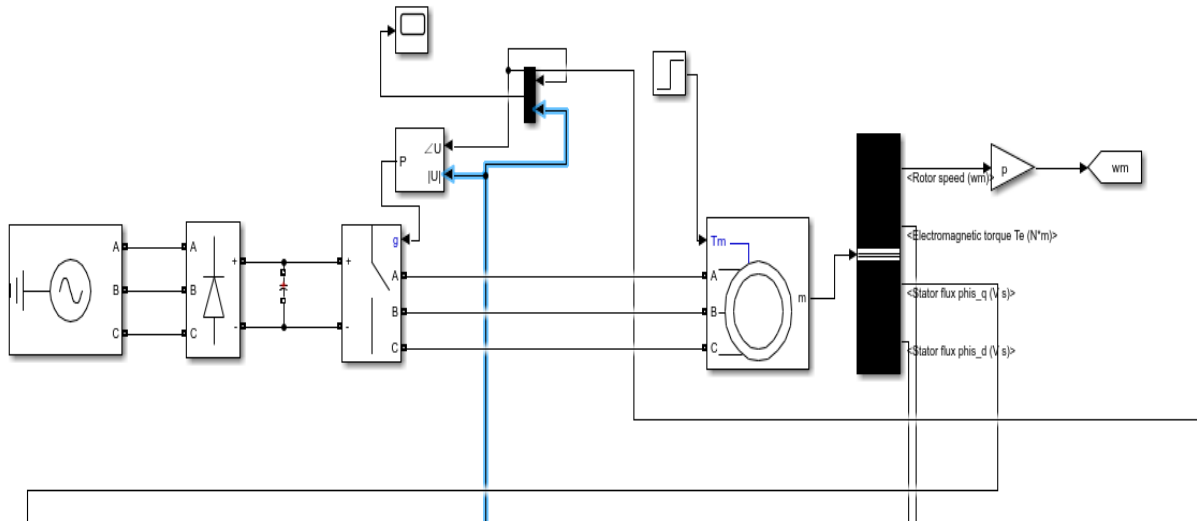
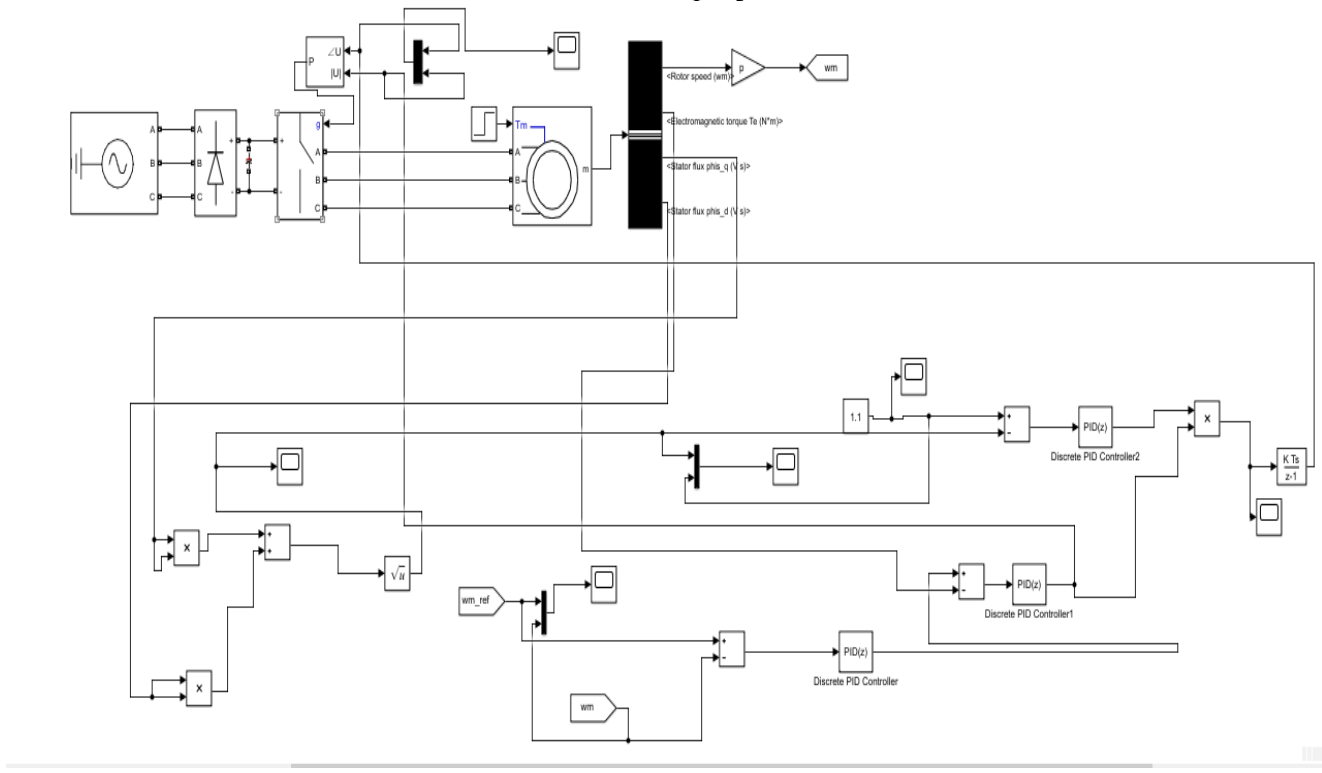
D-q model of the 3 phase induction motor (downloaded from mathsworks.com)



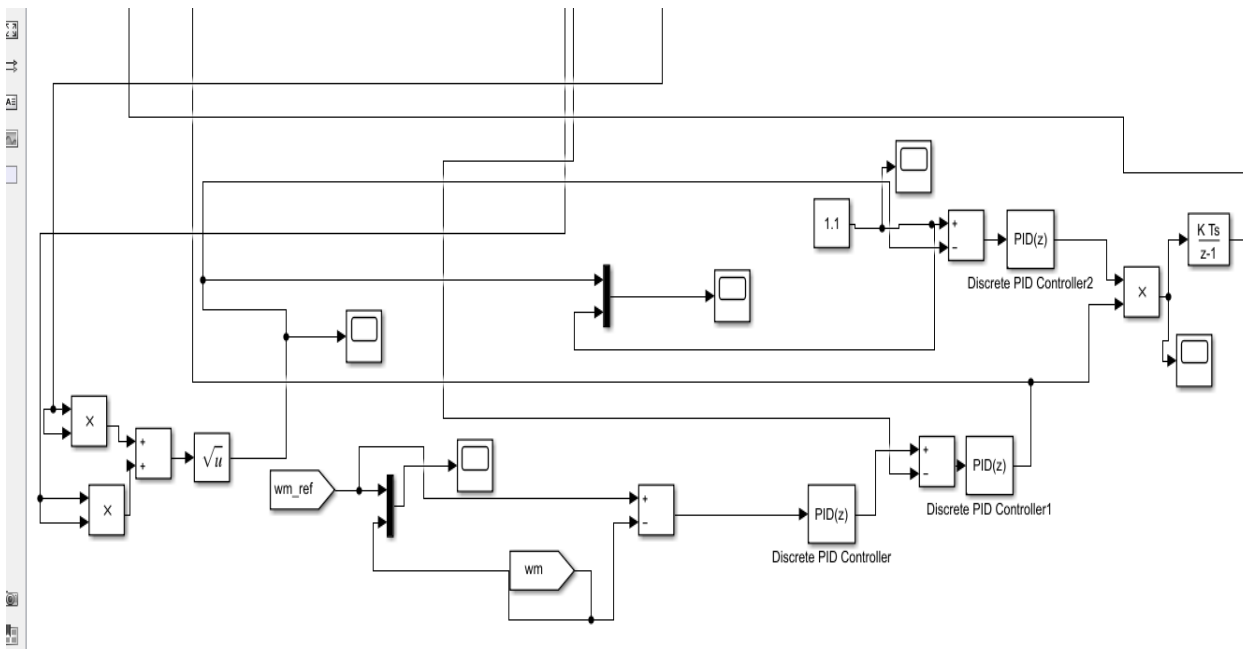
DTC with V/F control implemented in [23] which we want to duplicate:



The Simulink DTC with V/F Model constructed in our project:



Induction motor with SVPWM and three phase inverter with three phase source. Induction motor outputs the actual rotor speed, electromagnetic torque and stator flux according to the stationary reference frame. All of these variables will be used in the control loop.



Calculating the torque error and using PID controller will provide the Vsref and multiplying the flux error to achieve frequency/voltage then mulitplying by voltage to obtain the frequency then integrating it to achieve the stator phase, the same as the implemented control loop described above in [23].